Economic and design optimisation of a 15MW floating offshore wind platform using time-series forecasting

Craig White[1,3], Victor Benifla[2], José Cândido[1], Luís M. C. Gato[3]
[1] WavEC Offshore Renewables, Lisbon, 1350-352, Portugal
[2] University of Rostock, 18051, Rostock, Germany
[3] Instituto Superior Técnico (IST), Lisbon, 1049-001 Portugal

Correspondence to: Craig White(craig.white@wavec.org)

Abstract. ~~This work proposes a~~A structural and economic optimisation framework applicable to floating semi-submersible platforms, demonstrated here for a 15-MW offshore wind design, is presented. A genetic algorithm was developed that can seek a multi-objective solution to minimise mass whilst respecting the constraints of loads acting upon the system. Statistical and machine learning methods are then employed to forecast near and far term costs of the platform under a range ~~of~~ exogenous data scenarios, selected to support and boost forecasting accuracy alongside a hybrid forecasting method.~~.~~ Steel mass was reduced from 3916t to 3273t whilst respecting platform response constraints. The uncertainty of steel prices has the most significant impact on CAPEX, approximately €150-200M at 1GW level. ~~Finally,~~ Levelized Cost of Energy (CoE) is calculated to gauge the technical and economic viability, with 3-5€/MWh variation across forecasts.~~. Results show that a mass reduction of 9% is possible. With optimal costs predicted under the SARIMAX scenario of 4404.56€/t, 24.1% under the average. The optimised platform results in an LCoE reduction of 2.08%.~~

1 Introduction

The deployment of floating wind turbines (FOWTs) into deeper waters ~~offers access to stronger~~can harness improved wind resources with ~~better wind resources, with less~~reduced ~~-~~ marine competition and ~~lower~~ visual impacts. Floating technology has ~~witnessed rapid growth~~grown rapidly since the first full-scale prototype in 2009 (Skaare, et al., 2015), with pre-commercial status achieved in 2017 (Jacobsen & Godvik, 2021), 50MW in 2021 (Risch, et al., 2023) and 88MW in 2023 (Musial, et al., 2023), but growth has since stagnated. Costs have increased in the recent macroeconomic context and must decrease to achieve commercial ~~deployment in the hundreds of megawatts (MW)~~ gigawatt-level ~~and global installed~~ capacities~~ty~~ ~~in the hundreds of gigawatts (GW)~~ (DNV, 2023). ~~Key a~~Areas of cost-reduction potential should be ~~targeted first~~prioritised ~~whilst maintaining strong offshore reliability, energy production and availability~~ including ~~to ensure competitive levelized cost of energy (LCoE) which will boost successful auctions and deployment~~~~, with~~ the ~~floating platform~~floating substructure ~~being a promising area due to its large mass and high steel construction~~ (Barter, et al., 2020).~~.~~ Floating offshore wind (FOW) levelized cost of energy (LCoE) must reduce ~~must see LCoE reductions~~ to ~~become economically viable and~~ compete in auctions ~~with~~against ~~offshore wind and~~ other renewable energy technologies.~~, with the floating platform being a promising area due to its large mass and high steel construction~~ (Barter, et al., 2020)~~(Barter, et al., 2020).~~

Formatted: Portuguese (Brazil)
Formatted: Portuguese (Brazil)
Formatted: Portuguese (Brazil), Superscript
Formatted: Font: Not Bold
Formatted: Font: (Default) +Headings (Times New Roma
Formatted: Font: (Default) +Headings (Times New Roma
Field Code Changed
Field Code Changed
Field Code Changed
Formatted: Do not check spelling or grammar
Field Code Changed

This cost problem offers space for innovative solutions across three main platform areas: dimensions~~the dimensions of the platform itself~~, ~~the~~ cost and type of materials, and matching the design to site conditions.

~~Market prices for key raw materials, including steel, have witnessed high volatility in recent years. Methods to accurately predict future prices would reduce risk and improve strategic planning for developers to minimise costs and LCoE, especially for forecasts accurate from initial feasibility to final investment decision (FID) and procurement phase. Among these, time-series forecasting (TSF) methods using statistical, machine-learning, and neural network models offer promising solutions by looking back at past trends to predict future values.~~

~~Currently, floating offshore wind turbines (FOWTs) do not have a fully integrated system design from nacelle to anchor, and rely on conventional turbines attached to floating platforms.~~ There are currently four main designs of ~~platform that are yet to reach a mature and~~support structure which are yet to standardise ~~optimised standard~~ like fixed offshore wind monopiles and jacket foundations. ~~.~~Barges allows ~~for~~ concrete ~~and steel~~ construction ~~which lowers cost and can include a central pool~~and can dampen ~~to dampen~~ wave action and heave floater motions (Beyer, et al., 2015). Tension-leg platforms (TLPs) ~~(TLPs) offer low mass and draft due to the tension stabilisation of the mooring lines, which~~ transfer loads to the taut mooring and anchoring system, lowering platform mass. Spars are ballast-stabilised and have a simplified cylindrical design and higher draft. Semi-submersibles are buoyancy-stabilised ~~due to~~with a wider platform ~~and therefore~~which can operate in shallower waters. ~~This concept has higher mass and~~High volumes of steel ~~composition to achieve buoyancy stabilisation~~allow for ~~and can offer the opportunity for design minimisation through~~ geometry~~ical and thickness adjustments~~reductions to the structural steel components: namely the inner column, outer columns, pontoons and upper supports. This is true for –

~~R~~reference ~~turbines and~~ platforms that offer valuable standardised designs ~~that serve as a foundation~~ for ~~further~~ research and technology progression and provide a conservative layout, ~~with a minimised chance of failure~~ akin to prototype projects to ensure ~~maximum offshore~~ reliability.

Market prices for key raw materials like steel have witnessed high volatility in recent years, impacting CAPEX and project viability. Methods to accurately predict future prices would reduce risk and improve strategic planning for developers, especially for forecasts accurate initial feasibility to final investment decision (FID) and procurement. Among these, time-series forecasting (TSF) models using statistical and machine-learning methods offer solutions by looking at historical data to make future predictions. ~~. Due to its generic nature, the reference platforms serve as a basis for design improvements through geometrical adjustments to both the full system and sub-system components such as the columns and pontoons.~~

~~This is the purpose of this paper: to optimise both the design whilst ensuring that each design iteration adheres to acceptable levels of full-system load response, based on the environmental design conditions that reflect a range of realistic offshore scenario probabilities. The IEA reference 15MW wind turbine~~ (Gaertner, et al., 2020)~~(Gaertner, et al., 2020) is used alongside its partner UMaine reference Volturn-US-S (V-US) platform~~ (Allen, et al., 2020)~~(Allen, et al., 2020) for this study.~~This work implements TSF models to achieve a mass-minimised platform design by predicting commodity prices for the primary steel mass for strategic planning. A structural optimisation will iterate within the design space and defined

Formatted: Font: (Default) +Headings (Times New Roma
Do not check spelling or grammar

Field Code Changed

Formatted: Font: (Default) +Headings (Times New Roma
Do not check spelling or grammar

Field Code Changed

boundary constraints. The platform structural dynamic response in six degrees of freedom is examined using RAFT (Hall, et al., 2022) to maintain stability under a range of environmental load conditions. Price forecasts will be obtained using TSF models to achieve a mass-optimized platform CAPEX under a range of cost scenarios. The reference IEA ~~reference~~ 15MW wind turbine (Gaertner, et al., 2020) and ~~is used alongside its partner~~ UMaine reference Volturn-US-S (V-US) platform (Allen, et al., 2020) are used~~for this study~~.

2 Literature review

2.1 Floating platform: design, frequency response, and optimization

2.1.1 Support structure design

The main engineering challenge~~s~~ for FOW ~~require energy production whilst~~ maintaining stability in ~~a range of site conditions~~the marine environment whilst generating electricity. Nacelle motion, wave sensitivity and the mooring system footprint are outlined by (Butterfield, et al., 2005) and ~~point towards~~highlight how these challenges have already been overcome in the oil and gas ~~(O&G)~~ industry. These ~~requirements~~ challenges necessitated~~d~~ the development of frequency-domain codes that enabled~~, such as those used in this study for~~ rapid structural assessment across multiple design iterations. ~~A classification method is also presented for the variety of platform configurations into~~ They condensed designs into ballast, buoyancy, and tension stabilization, noting that in practice designs are hybrid~~ in nature,~~ and an optimal point ~~may be identified between all three,~~may lie between each type. ~~with se~~Serial production in high volumes ~~with~~ and onshore assembly also were found to offer~~ing~~ economic benefit. ~~If total platform cost reductions are within 25% then a competitive 0.05$/kWh could be reached, providing optimism for the industry and a snapshot of the favourable market conditions at the time of study.~~

Concept~~ual~~ and deployed semi-submersible ~~foundations~~s alongside~~, as well as~~ numerical simulation tools were reviewed ~~in~~ by (Liu, et al., 2016) and confirmed the same design classifications and ~~. The same three stabilization classification methods were employed as defined in the previous work by (Butterfield, et al., 2005). The focus on a semi-submersible design highlights the platforms potential through design~~its design simplicity and maturity ~~, and~~ justifies its selection ~~for analysis~~ in this study. ~~Three-legged, ring-shaped and V-shaped platforms, and the main numerical codes to investigate platform response to induced loads were discussed.~~

Due to the complexity and cost of ~~of full-scale testing at~~ sea testing, numerical modelling such as the ~~such as the~~ frequency-domain codes utilised in this ~~study,~~research ~~and tank testing~~ are preferable for ~~the research of~~ dynamic response studies.~~, with springs used to represent the catenary mooring system in scale testing.~~

~~The IEA 15MW reference wind turbine designed by (Gaertner, et al., 2020) forms the design basis for this research, and for the V-US floating platform. The turbine was produced with a view to future upscaling trends in offshore wind where turbine size constraints are not as strict as onshore.~~ The 15MW wind turbine ~~was seen as a~~follows other reference designs ~~natural follow-on from the DTU 10MW~~ (Bak, et al., 2013) ~~and 5MW NREL~~ (Jonkman, et al., 2009) and encompasses a threebladed rotor, Class IB direct-drive generator, variable-speed and collective pitch controller, a rotor diameter of 240m and a hub height of 150m. The turbine is designed for a fixed monopile foundation but has considerations and applicability for ~~floating studies~~FOW and follows the trend of using fixed offshore wind turbines ~~for additional use for FOW~~with thicker towers. The V-US floater (Allen, et al., 2020) ~~was designed to be paired with the~~is aligned ~~15MW turbine previously discussed to keep pace with the current offshore wind trend of ever larger wind turbines~~for larger 15MW turbines. ~~The platform is of steel construction with~~A steel platform connects three outer columns and pontoons ~~connecting~~ to a ~~narrower~~ central column that interfaces with the ~~connects to the wind turbine~~ tower ~~interface~~. All significant geometric values and ~~global~~ coordinates ~~link the~~allow design integration within ~~to aerodynamic, structural, and hydrodynamic~~ numerical models for analysis, such as those employed in this study.~~such as OpenFAST and RAFT that are used in this study.~~

Field Code Changed

As turbines increase in size offshore, scaling laws are important to model the impact of larger generators on platform size, with smaller increase in platform size supporting larger generators, improving LCoE. The study by (Papi & Bianchini, 2022) found ballasted mass increased 1.3 times for a tripling of power rating from 5-15MW. The generic upscaling methodology to transfer a FOW turbine geometry from 5MW-15+MW was proposed by (Wu & Kim, 2021), analysing the effects of changes to the column radius and floating base, which are also used in this research. Results showed that upscaling the column radius increased the overall mass and natural heave period, whilst upscaling the column distance raised the centre of gravity and metacentric height of the system, with a slight lowering of the natural heave period that is important for semi-submersible designs. These issues can be minimized through added ballast mass to lower the centre of gravity and increased added mass to raise the natural heave period. Ballast was maintained constant within this study to focus on the impact of structural steel changes.

2.1.2 Numerical models

~~To accurately model the response behaviour of a floating turbine to offshore loads, a~~All structural, aerodynamic and hydrodynamic ~~effects~~ loads should be considered when modelling the response behaviour of a floating turbine. ~~The coupled Dynamic Modelling of Floating Wind Turbine Systems~~A study by (Wayman, et al., 2006) investigated ~~- the methods to achieve this,~~ joining the structural and aerodynamics of the time-domain FAST with the numerical code of WAMIT for FOW systems in depths ranging from 10-200m. Coupled loads include the gyroscopic motion of the rotor on the ~~tower and floating platform~~system~~, and~~ and forces from wave excitation. Modelled motions were found to be acceptable ~~resulting from inputs including~~ with changing water depth and wind speed. ~~An economic analysis was also conducted alongside a detailed component-level costing which put the platform, moorings, and turbine install as key cost considerations. Of relevance to our presented study are the acceptable motions modelled at a similar depth range, and cost functions across multiple types, including per unit of distance, time and force. Final costs for the barge and TLP platform ranged from $1.4-$1.8 million respectively for a platform and mooring system, including installation for a 5MW system which shows the large range in platform costs.~~

The FAST model developed by the National Renewable Energy Laboratory (NREL) models the coupled response of floating wind turbines under realistic ocean conditions, validated ~~and was validated~~ with the Statoil-Hywind 2.3MW ~~demo~~demonstrator ~~floating wind turbine~~FOWT (Driscoll, et al., 2016). ~~Site~~ With metocean measurements main input variables, ~~formed the model input conditions and~~ the overall response of the platform and loads ~~acting on it were in good agreement~~agreed well with measured data and validated the model's performance ~~under these conditions and~~ for the ~~Hywind~~ spar~~-type~~ ~~foundation~~structure. ~~This, although in the time-domain helps to validate the use of numerical models to represent real offshore conditions and helped lead to the development of frequency-domain codes.~~

~~Frequency-domain models allow for faster analysis of a floating system's dynamic behaviour and a range of load conditions, without the need for simulations, and allows for multiple design iterations.~~ For FOW computationally efficient design optimisation, and utilised in this work, the Response Amplitude of Floating Turbines code (RAFT) looks to the full integrated system~~, rather than just the platform combined with time-domain turbine processing~~ (Hall, et al., 2022). ~~Here, co~~Co-design of the support structure, turbine and controller are modelled in the frequency domain for added computational efficiency and design improvements. Three reference FOW designs were modelled and were compared with ~~time-domain~~ OpenFAST simulations. The dynamic response spectra and statistics performed well and within an acceptable range ~~and within expected range~~ that verified the model's application to FOW studies~~ including this work~~.

A review of modelling techniques for floating offshore wind turbines (Otter, et al., 2021) reiterated the challenge~~s~~ of ~~the~~ strong coupling of the turbine aerodynamics and platform hydrodynamics. ~~, plus the Froude and Reynolds number scaling mismatch due to working with water and air fluid domains.~~ It highlights the move towards high-fidelity modelling due to the cost and complexity of physical testing~~ at scale~~, although not necessarily with CFD due to ~~the~~ long simulation times~~ times~~. The paper concludes that numerical modelling is a trade-off between accuracy and computational efficiency and that many numerical models require improvement, with CFD an option towards the end of the design phase. Physical testing can validate and calibrate numerical models and can be classed into full physical and hybrid testing, with the choice often down to phase, facilities, budget, and test uncertainties. A 3D finite element analysis (FEM) model for FOW support structures (Campos, et al., 2017) argued that common tools ignore the structural stiffness of the elements constituting the floating platform and are normally treated as rigid body. Flexibility was found to be crucial in structural lifetime analysis and this paper proposes a model to integrate the deformation of the structure within a fully coupled hydro-aero-servo-elastic time domain model. In the study presented here, computational efficiency is critical and a flexible-body finite element model is not the main focus. Multiple designs variants and load cases that impact the overall platform dynamics and system response would make a detailed structural assessment unfeasible at this stage. ~~This assertion is applicable to this work, running multiple design iterations and load cases.~~

Field Code Changed

Field Code Changed

~~Floater response~~

~~2.1.31.1.1 Floater response~~

~~The floater response governs the response of the floating platform to the loads acting on the structure.The influence of wakes and atmospheric stability on floater response by (Jacobsen and Godvik, Influence of wakes and atmospheric stability on the floater responses of the Hywind Scotland wind turbines 2021) studied the Hywind Scotland farm, in particular the wake interaction between turbines. Measurements of half of the six degrees of freedom that influence turbine motion (roll, pitch, yaw) were investigated and the wake effect of upstream turbines was found in the downstream devices. Atmospheric stability must be considered for offshore performance due to almost no wake effect observed under neutral and unstable conditions, but floater motions were found to be small at all studied wind speeds which credits the spar-shape design and suggests a future area of study for the presented method of analysis here.~~

~~A 3D finite element analysis (FEM) model for FOW support structures (Campos, et al., 2017) argued that common tools ignore the structural stiffness of the elements constituting the floating platform and are normally treated as rigid body. Flexibility was found to be crucial in structural lifetime analysis and this paper proposes a model to integrate the deformation of the structure within a fully coupled hydro-aero-servo-elastic time domain model. Hydrodynamic and aerodynamic loads are computed alongside the dynamic interactions between the turbine, structure, and internal forces. Results show good agreement between the model and experimental results, with maximum inclinations under 5º and nacelle accelerations 0.2g. FEM is not used in this work due to the computational resource and time required, but could be and interesting further study after a final optimised design.~~

2.1.3 Design optimization

~~Design optimisation~~

~~2.1.61.1.1 Design optimisation~~

The design optimization solves for an ~~desired~~ objective function ~~(~~such as platform ~~weight)~~mass by adjusting geometrical parameters whilst adhering to specified constraints. A complex reliability-based ~~design optimisation~~framework of a spar-type FOW support structure (Mareike & Kolios, 2021) coupled ~~is highly relevant when coupling~~ economic efficiency with design uncertainties. ~~, especially when classification and standardization is not available. This is more complex with floating turbines and this paper presented a framework to address this issue.~~ Environmental conditions, limits and uncertainties were specified and a reliability assessment ~~approach~~ defined ~~defined~~ which generated a response surface for various system geometries. ~~geometries in the design optimisation.~~ The ~~Using the example of a spar-type design, the~~ method met all constraints including the reliability criteria and reduced platform and ballast mass.

A software framework for a 22 MW Semisubmersible FOW platform (Zalkind & Bortolotti, 2024) was developed for the matching reference wind turbine ~~of the same capacity~~. ~~Different~~ Various fidelity levels and ~~the effect of varying~~ load cases

Formatted: No bullets or numbering

Formatted: Indent: First line: 0 cm

Field Code Changed

were evaluated for controller adjustment, plus the difference between sequential and simultaneous co-design. An algorithm that searches the design space before optimisation is suggested, and that solving smaller problems sequentially is advantageous rather than large simultaneous co-design solutions. Notwithstanding a more robust and reliable outcome, the simultaneous solution was found to produce a platform with 2% lower mass and therefore a trade-off between advantageous results and reliability is required. The current research also features a sequential optimisation for design, system load response, and economic analysis and similar system mass reduction results.

An efficient optimisation tool for floating offshore wind support structures (Faraggiana, et al., 2022) highlights the need for economic competitiveness through a reduction of the platform weight and therefore structural cost, matching the objectives of this paper with the same optimisation method albeit for a different platform. An optimisation tool applicable to any floating turbine is proposed that adjusts the geometry, in this case the OC3 spar-type design. The stability and dynamic performance were evaluated and optimised using a genetic algorithm (GA) coupled with a surrogate model to both minimise cost and maximise performance. Cost reductions across the best and worst cases of 2-3 times were found, with a 25% cost decrease between most and least restrictive optimal cases. Hydrostatic constraints were found to be more significant than dynamic ones due to influencing the design area.

Field Code Changed

~~As an optimal platform can be seen as a trade-off between weight and reliability, a multi-objective optimisation was developed (Qiua, et al., 2008) for three semi-submersible platforms using particle swam optimisation algorithm based on a surrogate model. Hydrodynamic performance was calculated using Morison's equation and the panel method, and the surrogate model was used to improve computational efficiency, with accuracy maintained using cross-validation. Platform weight and heave motion was selected as optimisation objectives, with metacentric height, surge motion and airgap as constraints. A multi-objective particle swarm method searched for optimal pareto fronts and was validated with a CFD tool. Heave motions could be reduced by 12.68-14.96% and total weight by 12.16-24.91%.~~

~~Genetic algorithm optimization~~

Formatted: List Paragraph,List Paragraph CV,cv list paragraph,List Paragraph1,Listenabsatz

Formatted: Indent: First line: 1.27 cm

The genetic algorithm is a useful tool which simulates natural reproduction and the fitness of certain populations to combine attributes and produce better offspring which help to achieve the objective function,~~.~~ allowing multi-objective analysis and design space visualisation. This makes GAs ideal for optimizing complex systems, such as FOW substructure designs, where optimisation involves different design variables, complex numerical models and non-linear constraints and reinforces the choice of optimization method in this study, involving multiple designs and load cases within a constrained optimization.

A global optimisation tool identified and evaluated the configuration of support structures for FOW (Hall & Buckham, 2012). The rationale highlighted the nascent stage of FOW optimisation and the complex nature of FOW system interactions in multiple mediums that inhibit the convergence of designs. Also, geometrical optimisation has previously omitted key design parameters which drives the need for a flexible GA approach. Results show designs similar in nature to established spar and

Field Code Changed

semi-submersible configurations, with others less conventional, and lead to the selection of the RAFT tool used within this work.

A GA framework was developed (Hall, et al., 2013) to optimize the support structure for FOW using a nine-variable parameterization, which is equal to the method employed in the current research. This broadened the design space further than the state of art that considered a frequency-domain dynamics model linearized forces that recreated the physical considerations acting on the turbine and support structure whilst remaining computationally efficient. The choice of GA allowed a visualisation of the design space and pareto front that showed optimal design choices, through minimization of both the support structure cost and root-mean-squared (RMSE) nacelle acceleration~~. Under $6 million, three outer cylinders is optimal and matches most currently deployed semi-submersible platforms, with six cylinders when costs rise above $6 million and heave plate size increasing with platform cost. The optimal complexity and unusual configuration of designs highlight improvements to the cost model to consider the added cost complexity of such designs.~~

~~In literature, evolutionary algorithms, particularly GAs, are widely used for FOWT substructure design optimisation by allowing multi-objective analysis and design space visualisation. These algorithms, inspired by biological evolution, operate with a population of individuals, each representing a potential design solution, which evolve through the design space. Genetic algorithms typically involve three main steps: selection, where individuals are chosen for the next generation or to produce offspring; crossover, where two parents are combined to create new individuals; and mutation, where random changes are introduced to maintain diversity. Each iteration, the fitness of the population is evaluated based on objective and constraint values, allowing the individuals to be ranked. While most follow this general procedure, there is significant flexibility in how these steps are implemented, leading to a variety of genetic operators and evolutionary strategies, which are well summarized by (Martins, 2022). GAs are extensively reviewed by (Sourabh Katoch, 2021), where different genetic operations and techniques are analysed. GAs are effective for both constrained and unconstrained optimisation problems, particularly when derivatives of the objective and constraint functions are complex to obtain. They are also well-suited for so-called "black box" optimisation problems, where the function to be optimized is obtained through complex numerical models requiring time-consuming simulations. This makes GAs ideal for optimizing complex systems, such as FOW turbine substructure designs, where optimisation involves different design variables, complex numerical models and non-linear constraints and reinforces the choice of optimization method in this study, involving multiple designs and load cases within a constrained optimization.~~

~~**2.1.7** Upscaling~~

~~As turbines increase in size offshore, scaling laws are important to model the impact of larger generators on platform size, with smaller additions to platform size able to support larger generators, improving LCoE. The generic upscaling methodology to transfer a FOW turbine geometry from 5MW-15+MW was proposed by (Wu & Kim, 2021), analysing the effects of changes to the column radius and floating base, which are also used in this research. Results showed that upscaling the column radius increased the overall mass and natural heave period, whilst upscaling the column distance raised the centre of gravity and metacentric height of the system, with a slight lowering of the natural heave period that is important for semi-submersible~~

Formatted: Indent: First line: 0 cm

Field Code Changed

Formatted: Normal, No bullets or numbering

~~designs. These issues can be minimized through added ballast mass to lower the centre of gravity and increased added mass to raise the natural heave period. A method of estimating the scaling of platform parameters was also provided for a range of turbine sizes and components. Ballast was maintained constant within this study to focus on the impact of structural steel changes.~~

~~A review of scaling laws applied to floating offshore wind turbines from 5MW-15MW (Sergiienko, et al., 2022) reiterates the upward trend in wind turbines and the need for platforms to also increase to support them. How the design and dynamics change with scale is investigated, with results showing that mass, rated power and rotor thrust scale close to the square of the rotor diameter, making it a useful consistent metric for parameter scaling with added rotor size. The paper also highlights that towers for FOW are usually thicker and heavier avoiding the wave excitation region matching the natural frequency, but for similar reasons were maintained constant in the work to focus on platform optimization. Regarding the platform geometry, there was a strong correlation found between the rotor diameter and the product of the offset columns and their diameter. Finally, design methods used by developers follow the square-cube scaling law when sizing platforms for larger wind turbines.~~

Formatted: Indent: First line: 0 cm

2.2 Economic analysis: Costs, LCoE, and forecasting methods

2.2.1 Costs and LCoE

~~2.2~~

Formatted: Normal, No bullets or numbering

~~1.1.1 Costs and LCoE~~

Feasibility of FOW ~~Floating Platform Systems for Wind Turbines~~ (Musial, et al., 2004) showed a technical description of several floating platforms classed by mooring system ~~method~~, especially ~~the contrast~~ between contrasting catenary and taut vertical systems. A cost comparison was made between a semi-submersible ~~tri-floater~~ and an NREL TLP ~~developed at NREL~~, both supporting a 5MW turbine. Production costs ~~are estimated at $7.1 million~~ for the semi-submersible ~~and $6.5 million for the NREL TLP. This~~ reduce~~s~~d by 40% ~~to $4.26 million and $2.88 million respectively~~ under structural optimisation. ~~, bringing the cost of energy to the US Department of Energy target of $0.05/kWh that the US Department of Energy necessary for large scale commercial FOW development.~~ Such reductions build the case for structural optimisation and its impact on LCoE~~, the goals of this current research~~.

Lifecycle LCoE perspective by (Myhr, et al., 2014) provided a detailed cost assessment of ~~multiple support~~the main discussed structures. ~~s including spar, semi-submersible, and TLP.~~ Mass-based calculations utilised in this research ~~that assisted the development of cost functions in this research for platform cost~~ were derived alongside the cost of mooring and anchoring systems, with depth and distance to shore found to ~~be a dominant factor in LCoE~~drive LCoE. ~~A large LCoE range of €82.0-€236.7 across substructures demonstrates the~~High ~~high~~ economic variability ~~and economic performance~~was found of designs, and the potential for cost reduction. Further work recommended progression of cost calculations to include scale~~ing~~ effects for mass-produced components ~~that is required for commercialisation of FOW,~~ and tailoring components and ~~overall~~ system design to site conditions, reflected in this research through varying load conditions.~~such as the varying load conditions presented here.~~

A systems engineering vision for FOW optimisation (Barter, et al., 2020) identified gaps to reduce the ~~cost of energy~~CoE, mainly through a ~~full~~ system-integrated approach to capture ~~the~~ complex interactions and physics across the lifecycle of a ~~floating wind~~FOW farm. A range of cost-reduction research areas ~~are~~ were outlined including new hybrid substructures, anchoring methods, two-bladed and/or downwind rotors, alternative materials and FOW-specific controls. ~~The paper argues that current engineering tools are inadequate to design systems that have cost-parity with the mature offshore wind sector. Flexible substructures, optimized turbine features and a geometry adaptive to the offshore environment are expected to be required. A multidisciplinary and multi-fidelity modelling approach that quantifies uncertainties is needed to achieve an optimal FOW system, and could inspire a future iteration of this research, taking the lower fidelity design gains into a higher fidelity analysis of promising platform designs.~~

~~High potential cost-reduction areas should be targeted first to drive cost reductions in FOW. These can be split into 'soft costs' such as financing and project management and 'hard costs' that mainly relate to physical components that comprise the floating offshore turbine, those aimed to be minimised within this current reseach.~~ These cost-reductions are realised through a combination of ~~economy~~ Economy of ~~scale~~ Scale (EoS) effects, improved learning rates ~~achieved through increased cumulative deployment~~ and design optimisation through research. ~~Areas of high potential for~~ FOW high potential areas ~~floating offshore wind (FOW)~~ were defined by (James & Ros, 2015), with ~~with a percentage reduction in costs from prototype to commercial scale. Installation is set for a 5% reduction, the balance of system (BoS) is expected to reduce by 9%, the turbine by 12% and~~ the floating platform highest with a 16% reduction in CAPEX from prototype to commercial scale, again reinforcing the focus on platform optimization.

2.2.2 Timeseries forecasting

~~This work implements both accurate TSF models alongside structural optimisation to achieve a cost-minimised platform design across both the design space and the time domain, by predicting commodity prices for key floating platform components for strategic planning over the next fifteen years. A structural optimisation will first create multiple layouts within the design space and defined boundary constraints. The chosen optimised layout that minimizes the platform mass will then have expected aerodynamic and hydrodynamic loads applied using RAFT (Hall, et al., 2022) to the structure to confirm its suitability for a given range of sites and conditions. The cheapest layout that withstands acceptable loads will then pass to the economic optimisation phase: The best point of material purchasing will be obtained using the TSF model, to achieve an optimized system in the space, frequency, and time domains.~~

Formatted: Indent: First line: 0 cm

Field Code Changed

Formatted: Font: (Default) +Headings (Times New Roma

Formatted: Normal, Indent: First line: 0 cm

~~2.2.2 Timeseries forecasting~~

~~Add section here~~Forecasting of time-series data, observations made sequentially though time, is crucial in the areas of science, industry, commerce and economics (Chatfield, 2020)~~, and~~. It can consist of forecasting just one time-series, or a group of either separate forecasts or grouped data which supports one forecast, ~~as is the case with this work~~as presented here. A variety of predictive regressive models can perform this task, with machine learning models able to capture complex patterns, and statistical models capturing seasonal and longer-term trends. A seasonal autoregressive model with exogenous variables (SARIMAX) model forecasted short-term electricity load in (Tarsitano & Amerise, 2017) which managed accurate predictions through dynamic regression, for a shorter timeframe of multiple days. Residuals de-trend the data and were supported by exog hourly loads and calendar effects. An eXtreme Gradient Boosting algorithm (XGBoost) used by (Zhang, et al., 2023) predicted energy and peak power for 1-3 years. Multi-step forecasting which includes recursive and sequential training, was employed to measure accuracy and stability. Hybrid combinations of these models, capture the benefits of each to produce accurate future predictions, as utilised in this work.

~~A floating~~The platform'~~'~~s steel shell costs ~~-~~are susceptible to market prices of primary and secondary steel, which have been highly variable in recent years (Albulescu, 2021) and especially after a global pandemic. ~~It is crucial that any forecasts~~Forecasts ~~are~~ must be statistically sound and ~~are~~ predicted with highest possible confidence. ~~-Forecasting of time-series data, observations made sequentially though time, is crucial in the areas of science, industry, commerce and economics~~ (Chatfield, 2020)~~(Chatfield, 2020), and can consist of forecasting just one time-series, or a group of either separate forecasts or grouped data which supports one forecast, as is the case with this work.~~ For specific commodity price forecasts, there is already research within statistics, machine learning, deep learning and neural networks that have already been applied to the platform materials studied in this work, namely steel. A method by (Wang, et al., 2020) into neural networks used a long short-term memory with exog ~~exogenous~~ features, with success in predicting trends over recurrent neural networks. The one-dimensional time series was restacked to enable period correction of seasonal features, by calculating and grouping data residuals as employed in the SARIMAX forecasts in this work.

Steel prices were ~~modelled~~ forecasted by (Jin & Xu, 2024) using gaussian process regressions. The model was trained using cross-validation and Bayesian optimizations, resulting in a low root mean square error (RMSE) of 0.54% between 2019 and 2021. Due to the structured data of most time series, machine learning and statistical models usually outperform more complex methods ~~especially~~ over longer timeframes, ~~and~~ with both methods ~~are~~ used within this ~~paper~~research. Accurate time-series forecasting could help inform procurement strategies, auction bids,~~y~~ and aid investor confidence with ~~for floating offshore wind and reduce~~lower risk~~,~~. But ~~however c~~care must be taken in model~~the~~ accuracy ~~of models~~ to ensure they are robust and to prevent access to actual data in the predictions during testing. This research has not been thoroughly applied within the context of steel for floating wind and presents a promising study area to explore.

Formatted: Indent: First line: 0 cm

Field Code Changed

Field Code Changed

Formatted: Do not check spelling or grammar

Field Code Changed

Formatted: Indent: First line: 1.27 cm

3 Method

This work can be divided into two main areas: First, ~~s. First the~~the platform mass minimization that is a combination of RAFT and a GA, which delivers a minimized mass that satisfies the overall constraints of the simulation. Second, the economic assessment that costs the floater based on ~~short to medium-term~~ forecasts of structural marine steel. Generalised project costs and power generation are then used to calculate the final LCoE over a range of future years to help strategize future floating offshore wind procurement.

3.1 Model for platform response and design optimization

The design of the V-US platform is composed of one central and three outer columns linked through pontoons and upper supports. Here, the design variables are continuous real values and defined as the main platform diameter (D), the centre and outer columns diameters (d_{cc}, d_{oc}), and the height, width and thickness of the pontoon (h_{po}, w_{po}, t_{po}), with parametrization highlighted in Figure 3. Any other design parameters for the substructure, mooring system, or turbine remain fixed with values from the base model.

The objective of this design optimisation problem is to minimize the total mass while ensuring its dynamic performance. The FOWT system is evaluated in terms of dynamic responses under a reduced set of load cases. While the environmental conditions in this study are not site-specific, they were selected based on experience values and previous design optimisation studies (Dou, et al., 2020) to represent typical conditions that need to be assessed for the development of FOWT substructures according to standards. Typically, these must include the rated wind speed of the rotor and harsh sea states to represent worst cases scenarios. Additionally, the three representative environmental conditions are chosen to reflect typical values for rated mean wind speed and sea state encountered in Europe, as seen in (Messmer, et al., 2023). It is also worth noting that there is no wind-wave misalignment and that the mean wind force is normal to the rotor plane.

Table 1 - Load conditions for design optimisation

	Units	LC 1	LC 2	LC 3	LC4	LC5	LC 6
Wind speed	Ws (m.s-1)	11	19	23	3	7	70
Sig. wave height	Hs (m)	1.10	2.04	2.85	6.3	8.0	10.68
Sig. wave period	Tp (s)	7.19	8.11	8.82	11.50	12.70	14.20
Operation state				Operating			Parked
Closest comparison with IEC DLCs	1.2	1.2	1.2	1.1/1.2	1.1/1.2	1.1/1.2	6.1

In this design optimisation study, the dynamic performance of the FOWT system is evaluated with constraints on specific aspects of the platform response and turbine behaviour. The maximum platform offset, the platform pitch, and the nacelle acceleration at the top of the tower in the wind direction are constrained ensuring these values remain within acceptable limits.

Finally, the fore-aft bending moment at the tower base and the static stress at the location at the interface between the central column and the pontoons are also considered and limited as they represent the stress that can be transferred to the substructure and is commonly limited in design. Each of these constraints values are computed for each defined load case and the maximum result across all cases is selected to be checked against the constraint limits of the optimisation problem. Defining these constraint limits to accurately represent real-world conditions can be challenging, so they are often set to general values based on experience. This approach is also applied here, supported by insights from previous optimisation and simulation studies and other publicly available models of the V-US.

~~3.1~~ The main inputs for the design optimisation study presented here are gathered and summarized in Table 1. Due to the inherent randomness of GAs the design optimisation problem is run 10 times to collect statistical results from multiple optimisation runs and properly assess the results and efficiency. For each run, the population starts at 100 individuals and the maximum number of generations is capped at 1000 for a reasonable amount of evaluation for this large design space.

Formatted: Normal, No bullets or numbering

3.1.1 Platform response

~~3.1.0 Platform response~~

The main objective is ~~in this first part is to perform~~ the ~~design~~ mass ~~optimisation~~ minimisation of a 15-MW semi-submersible platform. ~~To do so, the~~ The design optimisation framework presented in (Benifla & Adam, 2023) ~~is used and~~ was applied to the V-US substructure mounted with the IEA 15-MW reference offshore wind turbine (Gaertner, et al., 2020). In this study, the ~~Response~~ Response ~~amplitudes~~ Amplitude of ~~floating~~ Floating ~~turbines~~ Turbines (RAFT) open-source code is used to model the FOWT system in the frequency-domain and evaluate its static properties and dynamic response. The code has been validated against higher-fidelity tools such as OpenFAST and has shown good agreement while also being computationally efficient. This makes it an ideal choice for quickly evaluating various substructure designs under different environmental conditions (Hall, 2022).

Field Code Changed

Field Code Changed

In RAFT, the FOWT system is modelled as a rigid body with the common six degrees of freedom: surge, sway, heave, roll, pitch, and yaw. The dynamics are represented in the frequency domain, allowing the FOWT system to respond linearly to each excitation frequency. The complex amplitude of the system's response, X, at a given frequency ω, is obtained by solving the generic equation of motion for the FOWT system:

$$(-\omega^2 M + i\omega B + K)X(\omega) = F_{ext}(\omega), \qquad (1)$$

where, M, B, and K represent the FOWT system's total mass, damping, and stiffness matrices, respectively, F_{ext} the external excitation forces, and ω the frequency. The frequency-domain dynamics of the FOWT are assumed to operate around a specific position, $\overline{X}$, which represents the mean steady state of the system. This position is obtained by solving iteratively the static equilibrium equation derived from the previous equation:

$$K_h = \overline{F}_{ext} + \overline{F}_{moor}(\overline{X}), \quad (2)$$

where $\overline{F}_{ext}$ represents the mean external forces applied to the system, $\overline{F}_{moor}$ is the nonlinear reaction force of the mooring system (~~accounting for~~ the effective mooring stiffness), and K_h is the total hydrostatic stiffness.

In RAFT, the system can be evaluated under given environmental conditions defined by steady winds and stochastic sea states, characterized by a mean wind speed Ws and a JONSWAP wave spectrum with significant wave height Hs and peak period Tp. The rotor-nacelle assembly is modelled as a rigid body ~~and~~ with three identical blades ~~with~~ and specific dimensions (chord, twist angle, and prebend) and distributed aerodynamic properties (lift and drag coefficients). The tower is defined as a cylindrical member, and the floating substructure as a combination of interconnected members of different shapes, with mass, inertia, buoyancy, and hydrostatic stiffness obtained by summing individual contributions. Mean aerodynamic loads are computed using a steady-state blade-element momentum solver, while mooring forces are determined with a quasi-static solver. Stochastic events including turbulent wind fields, gusts, and extreme waves are of importance to aerodynamic and hydrodynamic loads acting on the system but are time-domain phenomena, incompatible to the frequency domain RAFT tool employed and the large number of design iterations and integration with the GA. The system's fast frequency response is obtained by linearizing the dynamic equations, accounting for rotor aerodynamics and hydrodynamic damping based on Morison's equation applied to discretized substructure strips. Finaly, RAFT computes the FOWT's mean offset and frequency-domain response, with maximum values estimated by combining the mean values and the complex response spectra. The maximum platform offset and other key quantities of interest—such as the tower-top nacelle acceleration and the tower-base bending moment in the fore-aft can be obtained. Different design load cases can be defined to include multiple wind and wave conditions, enabling a comprehensive evaluation of the system's dynamic response under various environmental scenarios.

Formatted: Indent: First line: 1.27 cm

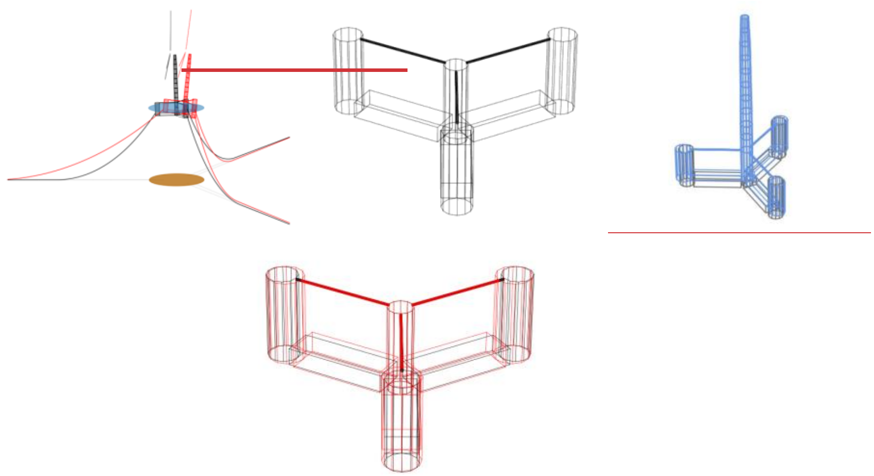

Figure 1 – a) RAFT model of the V-US and the IEA 15MW in its static position (black) and maximum offset (red)~~ when exposed to environmental conditions~~. b) ~~Original design of V-US~~Optimal system (blue) with tower, and c) Optimised platform design in red

Formatted: Caption, Indent: First line: 0 cm

A static stress analysis is performed to assess the structural integrity of potential designs. In this analysis the focus is at the ~~vulnerable~~ interface between the central column and pontoon. To estimate the loads, a free-body approach is followed, where the contributions of both the outer column and the pontoon itself are considered. Only considered here are structure weight and the buoyancy loads inducing moments on the structure interface. The stress σ on the pontoon base is:

$$\sigma = M \, {}^{h_{po}}\!/_{(2 \cdot I_{po})}, \tag{3}$$

where M is the total bending moment, and h_{po} and I_{po} are the height and second moment of area of the pontoon section.

3.1.2 Design optimization

~~3.1.0 Design Optimisation~~

The main objective is to reduce the steel mass of the V-US platform under several constraints to account for the dynamic of the system. For a given design solution, represented by x, the constrained single-objective optimisation problem can be:

Minimize:

$m(x)$

Subject to:

$$\begin{aligned} X_{Li} \le X_i \le X_{Ui} \quad & i = 1, \dots, n_x \\ g_j(X) \le g_{jlim} \quad & j = 1, \dots, n_g \end{aligned} \tag{4}$$

where m is the steel mass, X_{Li} and X_{Ui} denote the lower and upper limits of the design space and g_j is an inequality constraint with its associated limit g_{jlim}. These constraints are typically the output of the numerical analysis previously described that are monitored and constrained.

To solve, an efficient GA is implemented and inspired by (Hall, 2013). This was applied to FOWT substructure design, and addresses limitations of traditional evolutionary algorithms by identifying local optima and avoiding unnecessary problem evaluations. A distance-weighted scaling operation is performed to ensure that each local optimum identified within the population are treated equally. Throughout the optimisation, the fitness of the entire population is scaled, leading to the total scaled population fitness as described in (Hall, 2012). This is combined with a constraint-handling technique used by (Deb, 2000) allowing infeasible solutions to be compared solely based on their total constraint violation. This form of the penalty enables a clear comparison between feasible and infeasible solutions, allowing the GA to handle constraints effectively.

The initial population is generated and evolves by using Simulated Binary Crossover (SBX) and a polynomial mutation operation, originally introduced in (Deb & Agrawal, 1995). These efficient operators are widely used addressing real-valued optimisation problems. After new offspring are generated, they are assessed before being added to the current population. This ensures that they not too alike existing individuals while remaining close to fit ones. The check avoids the computational cost of evaluating the problem for individuals not added. This approach is particularly beneficial here, as evaluating the objective and constraint functions requires significant computational resources to run the numerical models described. It also ensures that the population evolves toward fitter regions of the design space, resulting in lower population density in less fit areas. The structure of the framework is shown in Figure 2~~Figure 2~~ and illustrates the interaction between the GA and the RAFT dynamic model.

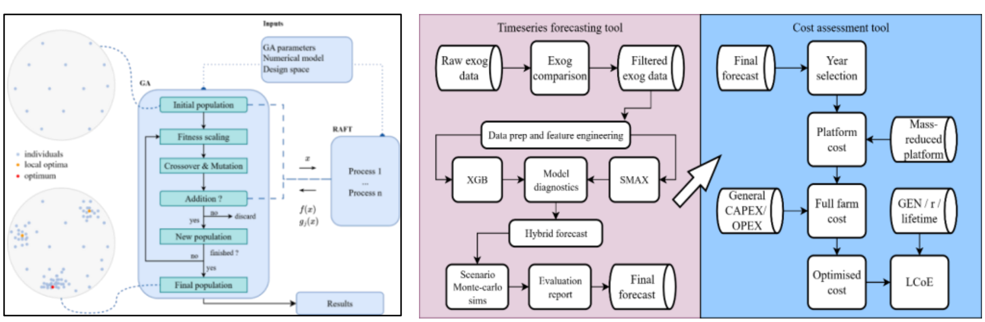

Figure 2 – Process flow of a) Design optimisation and b) Timeseries forecasting and cost assessment tool

3.2 Time series forecasting and economic assessment

After the design optimisation of the platform, an economic assessment is applied to the optimal~~e mass-minimised and constraint-respected~~ platform, and reference design~~structure~~. ~~First, a~~A range of future costs up to seven years ahead are forecasted using ~~various~~ a combination of forecasting methods. Second, these costs are applied to the final structure ~~mass~~ to derive a cost at platform and farm level, alongside an LCoE assessment.

3.2.1 Timeseries forecasting

~~**Time series forecasting**~~

The price forecasting tool incorporates~~is~~ a combination of models:~~,~~ a short-term ~~XGBoost (~~XGB~~)~~ which captures stochastics and fluctuation well, ~~model~~and ~~and~~ a statistical SARIMAX ~~(SMAX)~~ model better at capturing seasonality and long-term trends~~ for longer forecasts~~. The best performing singular or hybrid version was selected based on rolling hindcast testing windows~~. The output forecast selects the best model or a blend to capture stochastics and long/term trends to improve evaluation metrics which compare predicted and actual values in the test window~~. Both models rely on exog ~~exogenous~~ data ~~for~~ that are provided in the form of monthly prices, indices and other economic metrics. These supporting data are monthly time series of equal shape and granularity to the target predictor (HRC steel prices). They are external to the steel prices themselves but are linked (such as metals with impact on steel, metal indexes, energy prices, among others) which allow the predictor to build confidence. For. ~~that support steel price forecasts.~~ The equation the XGB total objective function $L\phi$ is:

$$L\phi = \sum_{i=1}^{n} I(y_i, \hat{y}_i) + \sum_{k=1}^{K} \Omega(f_k) , \qquad (5)$$

where $I(y_i, \hat{y}_i)$ the loss function between measured and predicted values, $\Omega(f_k)$ the regularization term which ~~penalise~~s complexity to reduce overfitting, f_k the k-th weakest decision tree learner in the group, and k the total number of decision trees.

For the SARIMAX model, finding the future steel price y_t when applied to a differenced stationary dataset is:

$$y_t = \mu + \phi(B)\Phi(B^S)(1-B)^d(1-B^S)^D y_t + \theta(B)\Theta(B^S)\varepsilon_t + \beta X_t, \qquad (6)$$

with μ the mean level of series, B the backshift operator defining the lags, for non-seasonal $(1-B)^d$ and seasonal $(1-B^S)^D$ differencing, $\phi(B)$ the nonseasonal and $\Phi(B^S)$ the seasonal autoregressive terms, $\theta(B)$ the non-seasonal and $\Theta(B^S)$ the seasonal moving average, ε_t the error term and βX_t the exog ~~exogenous~~ variables. The SARIMAX model simultaneously models the temporal behaviour of the steel prices and the influence of the selected external (exog) economic variables, allowing the prediction to be influenced by external market conditions and not just the past influence of steel prices.

Formatted: Font: Cambria Math

Formatted: Indent: First line: 1.27 cm

Candidate exogs $x_{t,}$ with the top-ranking group shown in Figure 3 are compared to the target steel prices $y_{t,}$ and filtered using statistical comparison metrics r (7), with monthly lag testing b (8) and rolling stability (9):

$$r(\Delta \log x_{t,} \Delta \log y_{t,}), \tag{7}$$

$$r(\Delta \log x_{t-b,} \Delta \log y_{t,}), \tag{8}$$

$$r_{t} = corr(\Delta \log x_{t,} \Delta \log y_{t})_{rolling}, \tag{9}$$

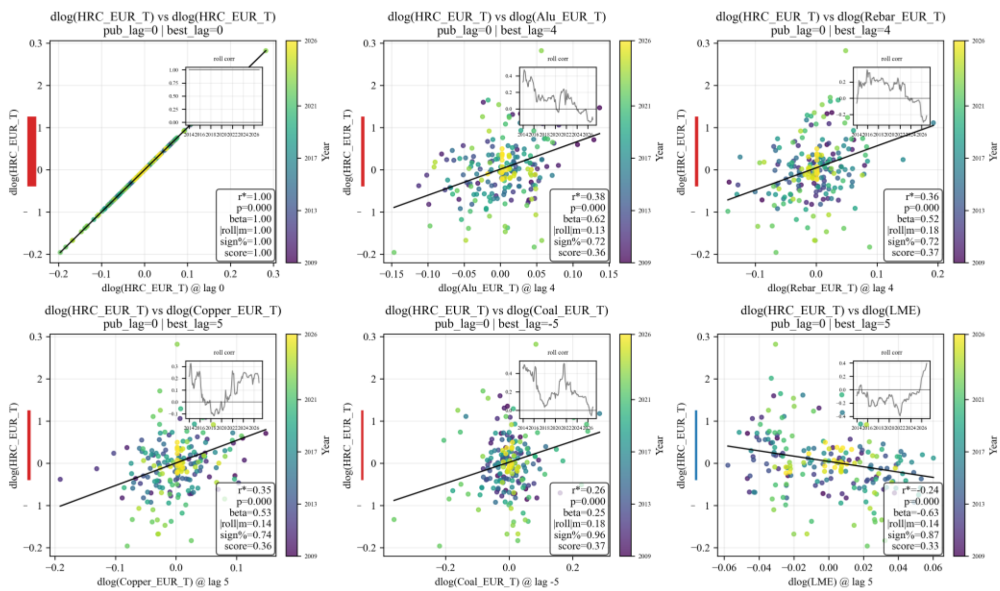

Figure 3 – Comparison of best performing exogenous data and target steel predictor data

~~The exogenous data was filtered using statistical comparison metrics including p/r value on a change log scale~~The best performing exog datasets are collected which pass multiple checks including stability, sign, mean strength, and lags, to create an optimum set of suitable supporting data for the forecasts and are shown in Figure 3. The x-axis shows the publication delay applied to the variable (months), and the y-axis the memory length (how many observations retained in the model). Red and

Formatted: Indent: First line: 1.27 cm

blue bars positive or negative trends, and thicker bars representing better performance. Multiple transformations (level, first difference, log-difference), lags and lengths are tested. Each exog receives a score based on the predictive strength, stability magnitude, and sign consistency. Only those that pass all thresholds and highest-ranked are stored in the final data group to boost prediction accuracy. Examples of the exog data passing the cross-correlation analysis with the target steel price are; rebar and copper acting as leading indicators; coal; London Metal Exchange LME). Such indicators are robust for inclusion into future steel forecasting.

The next phase transforms the exog data into $x_{t,}$ $\log x_{t,}$ and $\Delta \log x_{t,}$, then detrended with residuals where required, then ranked for usefulness, stability, and non-redundancy. Features including $\Delta \log(y_{t-1})$, $\Delta \log(y_{t-12})$, x_{t-b}, and x_{t-b-k} are then added, with b, k the best delay and memory term respectively, for the target $\Delta \log(y_{t,})$. The hybrid forecast $\hat{y}_{hy}$ combines the XGB and SARIMAX forecasts with two formulations: A weighted linear combination (10) with w the weight assigned to XGB, and a horizon-based regime switching method (11) with H the threshold horizon separating long and short term (3, 6, … months) h the forecast horizon in months:

$$\hat{y}_{hy} = w\hat{y}_{XGB} + (1-w)\hat{y}_{SAR}, \tag{10}$$

or

$$\hat{y}_{hy} = \begin{cases} \hat{y}_{XGB}, & h \leq H_{short} \\ \hat{y}_{SAR}, & x > H_{long} \end{cases}, \tag{11}$$

The final model is evaluated based on RMSE, mean absolute percentage error (MAPE) and symmetric mean absolute percentage error (sMAPE). ~~The best data from the comparison is then stored to aid predictions, with adjustable comparison criteria, usually on p-value significance measure. Data is then cleaned and aligned to create training and testing splits with the full process seen in Figure 2.~~

~~**The short-term machine learning XGBoost (XGB) model is used for the initial forecast, usually set to 12-36 months and selected due to an ability to understand stochastic short-term patterns in the data, as well as the acceptance of exogenous data akin to the SMAX model. Data protections are included so that the model is trained per horizon, and that it cannot cheat and see future data in the test section. Both models are evaluated based on a rolling cumulative validation, judged using Mean Average Error (MAE), Root mean squared error (RMSE) and model evaluation criteria: Akaike and Bayesian Information Criteria (AIC/BIC). The medium to long-term SMAX from the start of the forecast window but over a longer period, up to a maximum seven years. An optimisation loop finds the model parameters which deliver the lowest evaluation criteria akin to the XGB forecast. A hybrid forecast then combines the two, selecting automatically the best fitting model for each section, which generally is XGB for the first 12-24 months and then blended into SMAX which creates the forecast used to cost the semi-submersible platform. A final evaluation tests the forecasts against past windows with guards against data leakage, with added evaluation metrics to check the performance of the hybrid forecast.**~~

3.2.2 Economic assessment

Formatted: Indent: First line: 1.27 cm

Formatted: Caption, Indent: First line: 0 cm

Formatted: List Paragraph,List Paragraph CV,cv list paragraph,List Paragraph1,Listenabsatz, Keep with next

Formatted: Font: Not Bold

Formatted: Normal, None, No bullets or numbering

~~**Economic assessment**~~

The forecast monthly steel prices are first aggregated into yearly values $P_{y,s}^{HRC}$ and converted to marine grade steel for platform cost analysis, found from~~With a hybrid forecast defined for up to seven years, platform costs from literature~~ (BVG, 2025) ~~transform the HRC steel prices into platform cost data~~. Only the primary steel mass is impacted by the price forecasts in this study, which forms almost the entire cost. Steel is assumed to be purchased in a given year where contracts with the fabricator are agreed, it is not assumed that all units are purchased in that year.

Field Code Changed

$$P_{y,s}^{HRC} = \frac{1}{n_y} \sum_m \hat{P}_{m,s}^{HRC}, \qquad (12)$$

With $P_{m,s}^{HRC}$ the monthly predicted values, n_y the number of monthly observations and s the forecast scenario. Other platform components including secondary steel items, ballast and controls are costed from literature as other CAPEX, as they are not the main subject of this study and primary steel contributes around 83% of the total platform (BVG, 2025). The platform cost $CAPEX_{plat}$ can be found by:

Field Code Changed

$$CAPEX_{plat} = P_{y,s}^{marine} \cdot M_d \cdot N_p \qquad (13)$$

Formatted: List Paragraph,List Paragraph CV,cv list paragraph,List Paragraph1,Listenabsatz

With $P_{y,s}^{marine}$ the price of marine grade steel, M_d the mass of platform design and N_p the number of platforms, omitted for one platform. Total CAPEX is the summation of the platform CAPEX and all other CAPEX. Other wind farm costs are generalised ~~again~~ from (BVG, 2025) to remove site-specific and project bias, with primary steel mass of the platform removed to allow space for the optimised platform. A net capacity factor of 0.4925 that considers all losses including electrical are used for a floating offshore 1GW wind farm (Beiter, et al., 2020), validated with a gross CF of 0.5024 (Martini, et al., 2016) to arrive at an LCoE value per year of the forecast. LCoE is then placed within the current framework of to see how both the economic and structural design optimisation influence both platform cost and $LCoE$ ~~LCoE~~:~~.~~

Field Code Changed

Field Code Changed

Field Code Changed

$$LCoE_{y,s,d}^{€/MWh} = \frac{CAPEX_{y,s,d}^{total} + PV_{OPEX} PV_{DECEX}}{PV_E} \qquad (14)$$

With $CAPEX_{y,s,d}^{total}$ the total CAPEX for year y, PV_{OPEX}, PV_{DECEX}, and PV_E the present value of OPEX, DECEX, and energy generation respectively, discounted to present.

4 Results

4.1 Platform design

~~**Platform design**~~

~~The design of the V-US platform is composed of one centre and three outer columns linked through pontoons and upper supports. Here, the design variables are continuous real values and defined as the main platform diameter (*D*), the centre and outer columns diameters (d_{cc}, d_{oc}) and the height, width and thickness of the pontoon (h_{po}, w_{po}, t_{po}). This design parametrization is highlighted in Figure 3. Any other design parameters for the substructure, mooring system, or turbine remain fixed and their values are from the base model.~~

~~The objective of this design optimisation problem is to minimize the total mass while ensuring its dynamic performance. The FOWT system is evaluated in terms of dynamic responses under a reduced set of load cases. While the environmental conditions in this study are not site-specific, they were selected based on experience values and previous design optimisation studies (Dou, 2020) to represent typical conditions that need to be assessed for the development of FOWT substructures according to standards. Typically, these must include the rated wind speed of the rotor and harsh sea states to represent worst cases scenarios. Additionally, the three representative environmental conditions are chosen to reflect typical values for rated mean wind speed and sea state encountered in Europe, as seen in (Messmer, 2023). It is also worth noting that there is no wind-wave misalignment and that the mean wind force is normal to the rotor plane.~~

Formatted: Indent: First line: 0 cm

~~Table 1 - Design load conditions for design optimisation~~

~~In this design optimisation study, the dynamic performance of the FOWT system is evaluated with constraints on specific aspects of the platform response and turbine behaviour. The maximum platform offset, the platform pitch, and the nacelle acceleration at the top of the tower in the wind direction are constrained ensuring these values remain within acceptable limits. Finally, the fore-aft bending moment at the tower base and the static stress at the location at the interface between the central column and the pontoons are also considered and limited as they represent the stress that can be transferred to the substructure and is commonly limited in design. Each of these constraints values are computed for each defined load case and the maximum result across all cases is selected to be checked against the constraint limits of the optimisation problem. Defining these constraint limits to accurately represent real-world conditions can be challenging, so they are often set to general values based on experience. This approach is also applied here, supported by insights from previous optimisation and simulation studies and other publicly available models of the V-US.~~

~~The main inputs for the design optimisation study presented here are gathered and summarized in Table 1. Due to the inherent randomness of GAs the design optimisation problem is run 10 times to collect statistical results from multiple optimisation runs and properly assess the results and efficiency. For each run, the population starts at 100 individuals and the maximum number of generations is capped at 1000 for a reasonable amount of evaluation for this large design space. The following figure shows the steel mass evolution of the best individual in the population through its evolution for all the runs. This shows the good behaviour of the algorithm that minimize the objective while reaching feasible regions of the design space where constraints are respected.~~

Formatted: Indent: First line: 0 cm

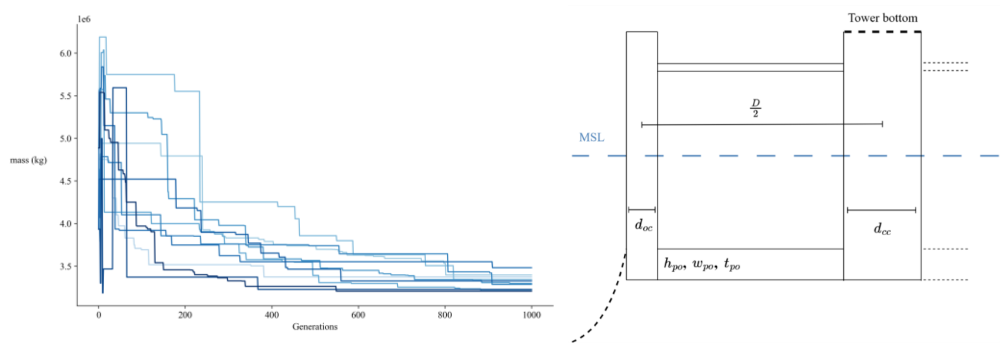

Figure 4

Formatted: Caption, Space After: 0 pt, Don't keep with n

~~Figure 3~~ – a) Mass/objective evolution for multiple runs b) Cross section of substructure and design parameters

The steel mass evolution of the best individual in the population through its evolution for all the runs is presented in Figure 4. This shows the algorithm's performance in minimizing the objective while reaching feasible regions of the design space where constraints are respected. The statistical results collected from the 10 optimisation runs showed consistent performance, with small standard deviations and some small variation between ~~the~~ run outputs. These results also shows that the algorithm led to near optimal solutions in some runs highlighting the importance of repeated optimisation. Out of all the runs, the chosen optimized design is gathered and compared with the base model shown in Figure 1~~Figure 1~~ (black base, optimised red) and the following Table 2~~Table 2~~. The worst successful design is chosen for the rest of this work so that it constitutes a safety margin that encapsulate some of the aspect neglected here. As expected, the mass is minimized while keeping the dynamic behaviour of the system as well as its structural integrity. The optimized mass obtained can be considered quite low when compared to the original, but this is anticipated as the structural check of potential designs is relatively simple here and lacks more in-depth analysis of the structure behaviour in terms of dynamic stress analysis. Mainly the optimized design exhibit slightly larger outer columns and pontoon dimensions but with a smaller platform diameter. Indeed, the design optimisation work presented here allows for a first optimized design that can be considered in the subsequent economic analysis. For further detailed analysis, once could consider other environmental analysis design space and enhance structural analysis to reach more confidence in the final optimize design.

Table 2 – Main characteristics of platform design and loads

	~~Symbol~~	~~Units~~	~~Bounds~~	~~Original~~	~~Optimized~~
~~Diameter~~	~~D~~	~~m~~	~~[50, 150]~~	~~103.5~~	~~100.46~~

Formatted Table

~~Diameter (central col)~~	~~D_{cc}~~	~~m~~	~~[10, 30]~~	~~10~~	~~10~~
~~Diameter (outer col)~~	~~D_{oc}~~	~~m~~	~~[5, 30]~~	~~12.5~~	~~14.46~~
~~Pontoon width~~	~~w_{po}~~	~~m~~	~~[5, 15]~~	~~12.4~~	~~13.98~~
~~Pontoon height~~	~~h_{po}~~	~~m~~	~~[5, 15]~~	~~7~~	~~8.58~~
~~Pontoon thickness~~	~~t_{po}~~	~~m~~	~~[0.001, 0.1]~~	~~0.05~~	~~0.032~~
~~Mass~~		~~t~~	~~-~~	~~3916~~	~~3611~~
~~Offset (m)~~		~~m~~	~~[0,25]~~	~~23.13~~	~~22.7~~
~~Pitch (°)~~		~~°~~	~~[0,5]~~	~~5.7~~	~~4.83~~
~~Tower bending moment~~		~~MNm~~	~~[0,600]~~	~~496.89~~	~~553.11~~
~~Nacelle acceleration~~		~~m/s²~~	~~[0,3]~~	~~1.76~~	~~2.12~~
~~Sigma~~		~~MPa~~	~~[0,300]~~	~~161.8~~	~~299,8~~

Parameter	Units	Limits	Original	Optimised	% reduction
Diameter	m	[50, 150]	103.5	108.8	5%
Draft	m	[15, 40]	20	15	-25%
Diameter outer col	m	[10, 30]	12.5	13.1	5%
Height pontoon	m	[5, 20]	7.00	5.56	-21%
Width pontoon	m	[5, 20]	12.40	8.66	-30%
Shell mass	t		3916	3273	-16%
Platform offset	m	<25	23.16	24.82	7%
Pitch	º	<5	5.70	4.98	-13%
Nacelle acceleration	m/s²	<3m	1.76	1.78	1%
Stress	Mpa	<300	161.8	205.0	27%

4.2 Timeseries forecasting

The ~~actual,~~ XGB, SARIMAX, and hybrid forecasts are shown in ~~Figure 4~~ Figure 5 for the model tested on hindcast data, running sequentially for 3-year phases. Model performance over the testing period 2022-2024, a period of high market fluctuation, improves with both hybrid forecasts and with the addition of exog data. Without supporting exog data to boost the prediction accuracy, the predicted values remain above actual prices and do not revert to the mean, with the price floor now raised due to the observed price spike in 2020 and cannot be considered a reliable baseline forecast. With exog supporting data, the SARIMAX forecast is continual decay in response to the 2022 price drop, showing a negative systematic price prediction bias. The hybrid model, selecting the best option for each predictor step, also adds accuracy to the model. The best performing exog supporting data (including other metals, indexes, and indicators, collected into the greatest hits collection of supporting data) produces the best testing results of 187.5 Mean Averaged Error (MAE) and shows the model's improvements when adding support and blended forecasting, and present a suitable candidate for future baseline scenarios.~~, with actual HRC steel price data running from 2009-2025, and the forecasts from 2025-2032. Seven years was deemed suitable for forecasts~~

Formatted: Font: Not Bold

Field Code Changed

Formatted: Font: Not Italic

Formatted: Font: Not Italic

Formatted: Font: Not Italic

Formatted: Font: Not Italic

Formatted: Font: Not Italic

~~due to the difficulty in obtaining long term forecasts, especially for volatile commodities. Also, most floating offshore wind procurement schedules at commercial-scale are expected to the be from four to seven years which was the ideal range for this study. The SMAX forecasts was trained using an 80/20 train/test split as was the XGB model. SAMX forecast is the most optimistic price-wise and also most sensitive to model changes which are inherent to achieving reliable forecasts, including seasonality, differencing, and others. With long computational times. The recent market volatility can be seen in the peaks within the data, decaying over time but with an overall dip in prices until 2030. For XGB, it is the most pessimistic of predictions, expecting higher prices that have small peaks and generally climb until the end of the forecast period in 2032. The hybrid is not necessarily the average of the two forecasts, and selects the best forecast on a rolling evaluation window. As the model does blend the forecasts, above with an overall 50-50 split, the hybrid is almost a mean value that serves as mid-point scenario in this study.~~

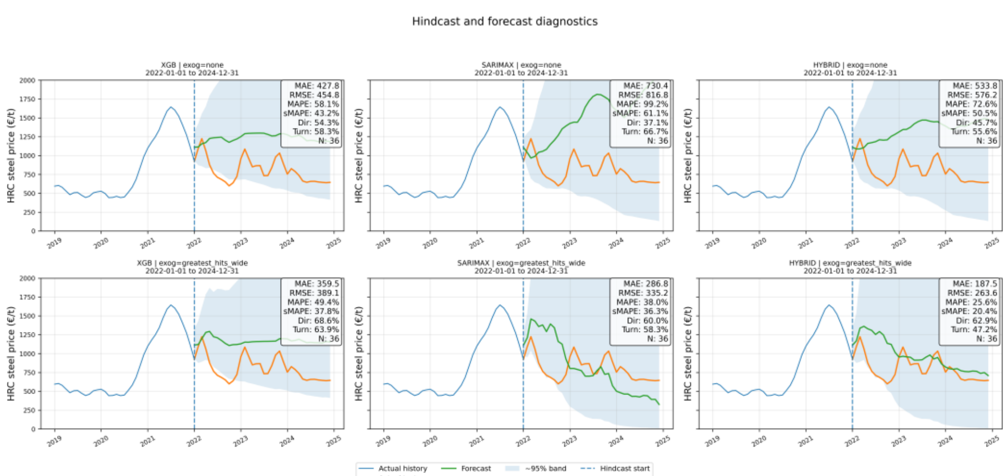

Figure 5 – Hindcast diagnostics of real and forecasted data for varying models and exogenous supporting data

Formatted: Line spacing: single, No bullets or numbering

~~**Time series forecasting**~~

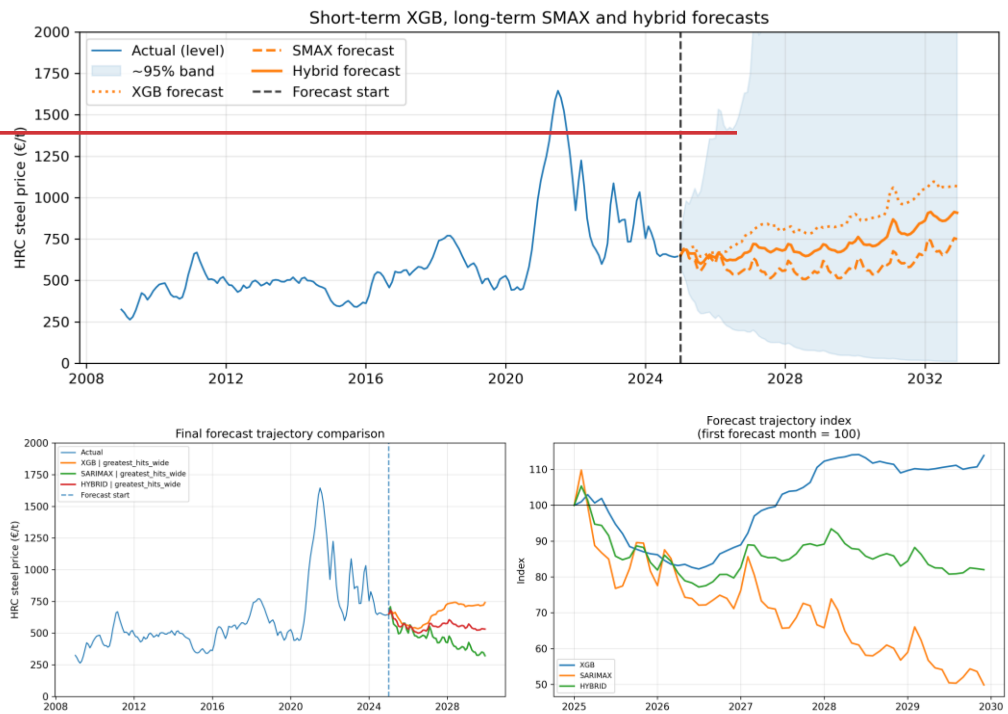

Figure 6

~~Figure 4~~ - **Short to long-term forecasts of HRC steel prices using XGB, SARIMAX ~~SMAX~~ and hybrid forecasts**

The future predictions ahead of current data after hindcast testing are presented in Figure 6. The XGB forecast recovers prices after an initial drop and can be considered a market recovery scenario, with a rebound of 10-15% showing no continual drift. The SARIMAX forecast up until the end of 2029 shows continual downwards drift which could be due to a lack of data transformation before forecasting. The hybrid forecast, alongside the best exog collection provides a balanced path and a moderate forecast which would be suitable for baseline projections, with the other two models providing upper and lower bounds.

Formatted: Keep with next

Formatted: Caption

Formatted: Normal

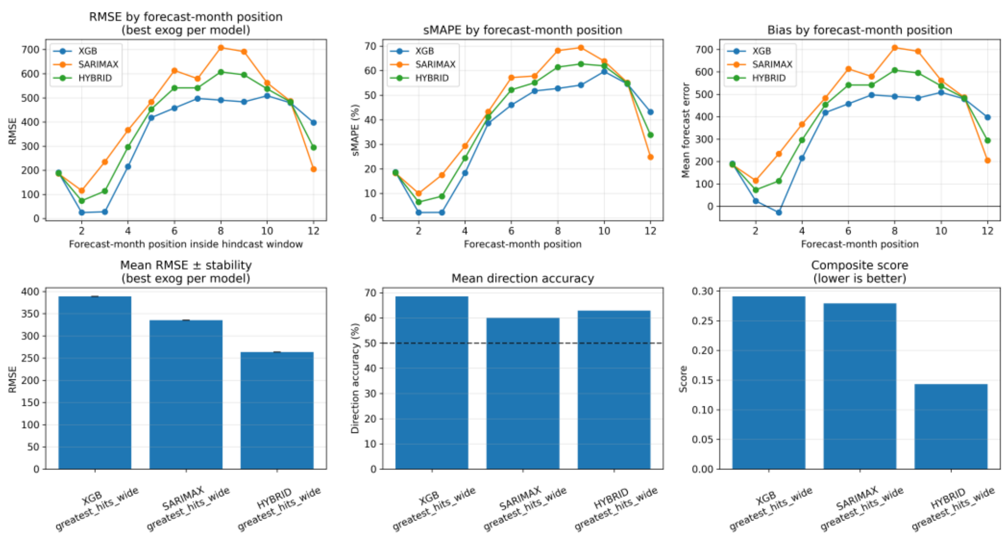

Figure 7 - Forecast month analysis and model performance ~~The actual, XGB, SMAX, and hybrid forecasts are shown in **Figure 4**, with actual HRC steel price data running from 2009-2025, and the forecasts from 2025-2032. Seven years was deemed suitable for forecasts due to the difficulty in obtaining long term forecasts, especially for volatile commodities. Also, most floating offshore wind procurement schedules at commercial-scale are expected to the be from four to seven years which was the ideal range for this study. The SMAX forecasts was trained using an 80/20 train/test split as was the XGB model. SAMX forecast is the most optimistic price-wise and also most sensitive to model changes which are inherent to achieving reliable forecasts, including seasonality, differencing, and others. With long computational times. The recent market volatility can be seen in the peaks within the data, decaying over time but with an overall dip in prices until 2030. For XGB, it is the most pessimistic of predictions, expecting higher prices that have small peaks and generally climb until the end of the forecast period in 2032. The hybrid is not necessarily the average of the two forecasts, and selects the best forecast on a rolling evaluation window. As the model does blend the forecasts, above with an overall 50-50 split, the hybrid is almost a mean value that serves as mid-point scenario in this study.~~

Formatted: Keep with next

Formatted: Line spacing: single

Formatted: Caption

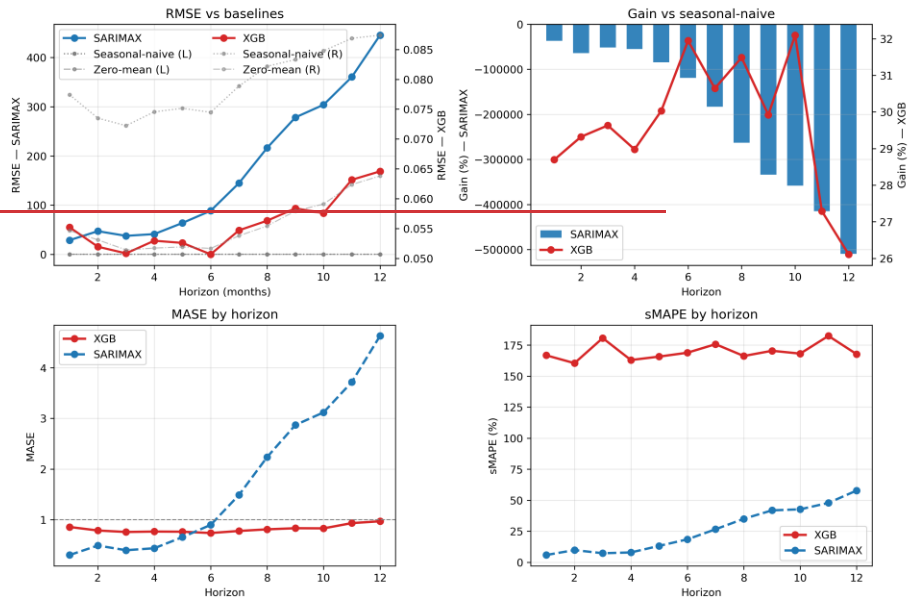

Formatted: Caption, Don't keep with next

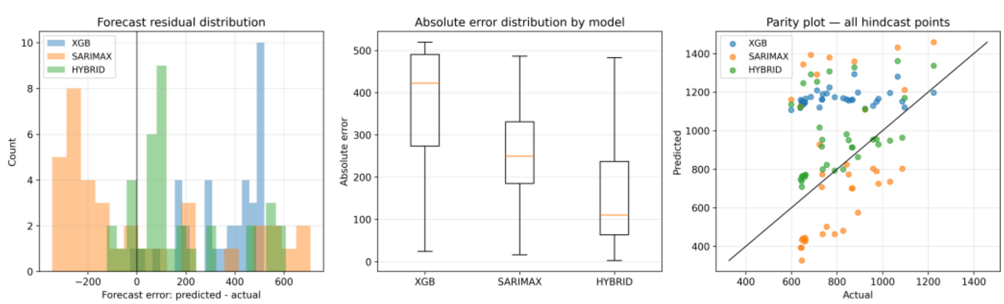

Figure 8

Formatted: Caption, Don't keep with next

~~Figure 5~~ - **Diagnostic analysis of XGB and** SARIMAX ~~SMAX~~ **forecasts** ~~**against the seasonal-naïve forecast**~~

The error structure by month position is shown in Figure 7 and shows all models as expected worsen with horizon, especially the SARIMAX forecast with a large spike in RMSE, symmetrical mean absolute percentage error (sMAPE), and mean forecast error. sMAPE measures the average relative difference between observed and forecasting values, treating over and underprediction equally. The XGB has higher overall stability but still performs worse than the hybrid forecast, which produce the lowest MAE during the hindcast test period and held relatively low root-mean-squared-error (RMSE) and sMAPE, with a mean bias (or average forecast error) close to zero. It provided the most consistent performance across the defined metrics Interestingly and unexpectedly, SARIMAX performs best in the short-term and seems errors rise with the negative forecast bias. However, this could be due to more data preparation or transformation. An evaluation of the XGB, ~~and~~ SARIMAX, and hybrid ~~SMAX~~ models against the actual hindcast data -can be seen in Figure 8 ~~Figure 5~~. In support of the hindcasts testing results, the hybrid model again proves most valuable, with lower forecast errors, error and a tighter spread of data points closer to actual results, with residuals centred around zero. The XGB has a positive bias through overestimation from, with the SARIMAX the opposite with a tendency for underprediction. ~~, with good model performance against the seasonal naïve with lower root mean square error (RMSE), especially for the XGB and better performance. It is expected for RMSE to climb towards the end of a forecast period but this is more sudden for the SMAX model. The XGB model is more stable and at this stage a more reliable predictor, with the SMAX forecast performing better at shorter forecasts. Overall, the models perform better than the baseline repetitive forecasts which does not change over time, the SMAX model requires further tuning for long term forecasts or perhaps different exog data.~~

4.3 Economic assessment

~~**Economic assessment**~~

The steel price and LCoE with changing forecast year are shown below in- Figure 9~~Figure 6~~, for the three scenarios and for the two types of platform: Initial ~~(ini)~~ mass of 3916~~2~~t and o~~O~~ptimised ~~-(opti)~~ 3273t~~481~~, around 10-15% savings across scenarios and which is the best and consistent outcome from the GA model. With the predictions affecting only steel prices, the CAPEX trends follow the same path as in the forecasting results, With XBG and SARIMAX the high and low bounds forecasts, and hybrid the baseline scenario. The uncertainty of steel prices has a significant impact on CAPEX, approximately €150-200M at 1GW level, or by up to 40-50% variation across the range of forecasts. Based on these results, market factors are a primary driver of economic uncertainties, with engineering optimisation offering significant yet partial mitigation.~~As the platform cost is applied across the forecast window consistently, results follow the trend of the three predictions with SMAX offering a minimised steel price (marine-grade) of under €4500/t in 2028, with LCoE at around 162-166€/MWh depending on platform optimisation. With the platform mass reduction resulting in LCoE savings of approximately 2.08%, with the biggest gap occurring during the XGB forecast. All three scenarios do show an overall upwards trend in steel price in the medium to long term, with SMAX prices starting to climb from 2029 onwards.~~

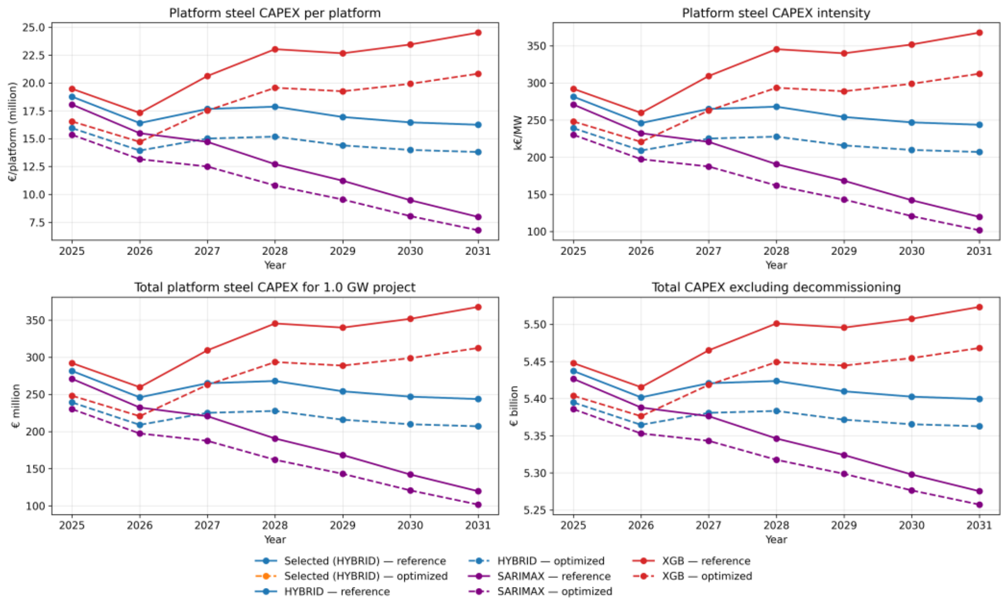

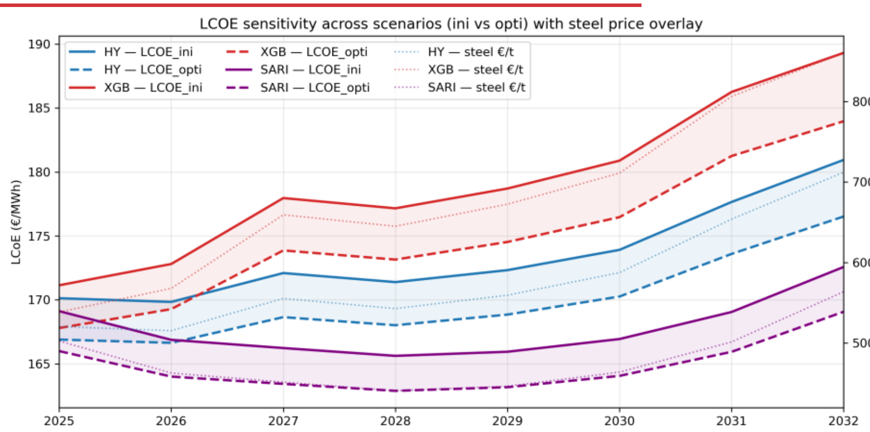

Figure 9-

~~Figure 6 – Platform total cost~~Total cost per platform, per project and for total CAPEX~~ and LCoE for platform and forecast type~~

Formatted: Caption, Don't keep with next

For LCoE as shown in Figure 10 shows a more moderate impact, around 3-5€/MWh with effects lessened through a long project lifetime of 30 years and higher discount rates of 8% to reflect early-commercial FOW projects, with structural optimization reducing LCoE by around 1€/MWh and more significant in the high-price scenarios. LCoE values are also encompassing other CAPEX items, energy generation, and OPEX, which were all generalised in this work.

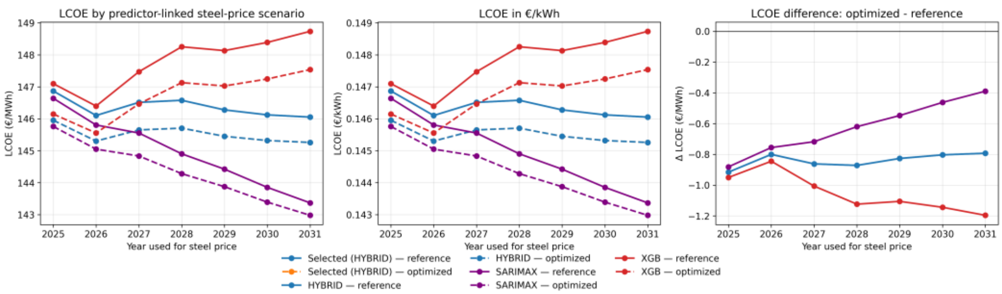

Figure 10 – LCoE analysis of the three models and optimized and non-optimized systems

5 Conclusions

This work presented the combination of a platform ~~mass minimization~~design optimisation whilst respecting design constraints, and a techno~~-~~economic assessment that ~~costed the platform~~calculated the platform and project CAPEX ~~now and into the future~~ using a combination of forecasting methods. The LCoE was estimated using general costs and energy generation from wider literature, which placed the system within both a 1GW farm scale and within the current LCoE framework. Results show that design improvements are possible for the reference platform whilst still respecting the constraints of expected loads acting on the floating turbine in the offshore environment, with savings of 10-15% in steel shell mass.~~.~~

For cost forecasting, it is possible to blend forecasts to take advantage of the benefits of short-term models that can capture stochastic fluctuation, ~~and also~~ longer-term statistical models that can capture deeper trends in time-series data. In this research the hybrid model outperformed XGB ~~outperformed the~~and SARIMAX ~~SMAX~~ model by capturing the benefits of both and combined they form three scenario forecasts. As SARIMAX conversely performed best in early forecast months, ~~and~~ more calibration is required to build confidence in future predictions. This work highlights the promising nature of predictive models, especially with selection of supporting data through filtering and wider economic analysis. Overall, the market fluctuations are strong drivers of platform CAPEX with €150-200M at 1GW level, or 40-50% fluctuation across all scenarios, and 3-5€/MWh LCoE. This shows economic forces are strong drivers of CAPEX and LCoE for a high priority cost reduction area for floating offshore wind. These, alongside the benefit of design optimization measures, must reduce for commercial potential to be realised. ~~The models did however perform better than seasonal naïve forecasts which assume no change and give promise to the ability to predict future commodity prices that can help inform the procurement process and development of floating offshore wind.~~

Formatted: Normal

Formatted: Keep with next

Formatted: Font: Not Bold

6 Data availability

The RAFT code is available at https://github.com/WISDEM/RAFT (last access: 27 July 2026), DOI 10.1088/1742-6596/2265/4/042020. The genetic algorithm used for the design optimisation is available at https://github.com/vbenifla/VikOpti/tree/main. Code for timeseries forecaster is available at https://doi.org/10.5281/zenodo.21631992

7 Author contributions

Economic analysis and time series forecasting code development and writing by Craig White. Platform design optimisation, simulations, development of genetic algorithm and writing by Victor Benifla. Results and manuscript review by José Cândido. Assistance with submission and support by Luís M. C. Gato.

8 Competing interests

The contact author has declared that none of the authors has any competing interests.

Formatted: None, No bullets or numbering

Formatted: Font: Not Bold

Formatted: None, No bullets or numbering

Formatted: List Paragraph,List Paragraph CV,cv list paragraph,List Paragraph1,Listenabsatz

~~References~~

~~Albulescu, C. T., 2021. COVID-19 and the United States financial markets' volatility. Finance research letters, Volume 38.~~

~~Allen, C. et al., 2020. Definition of the UMaine VolturnUS-S Reference Platform Developed for the IEA Wind 15-Megawatt Offshore Reference Wind Turbine, Golden, CO: National Renewable Energy Laboratory.~~

~~Bak, C. et al., 2013. The DTU 10-MW reference wind turbine, Copenhagen/Roskilde: Danish wind power research.~~

~~Barter, G. E., Robertson, A. & Musial, W., 2020. A systems engineering vision for floating offshore wind cost optimization. Renewable Energy Focus, Volume 34.~~

~~Beiter, P. et al., 2020. The cost of floating offshore wind energy in California between 2019 and 2032, Golden, CO (United States).: National Renewable Energy Lab (NREL).~~

~~Benifla, V. & Adam, F., 2023. Design Optimization of Floating Offshore Wind Turbine Substructure Using Frequency Domain Modelling and Genetic Algorithm. Trondheim, s.n.~~

~~Beyer, F., Choisnet, T., Kretschmer, M. & Cheng, P. W., 2015. Coupled MBS-CFD simulation of the IDEOL floating offshore wind turbine foundation compared to wave tank model test data.. ISOPE International Ocean and Polar Engineering Conference.~~

~~Butterfield, S., Musial, W. & Jonkman, J., 2005. Engineering Challenges for Floating Offshore Wind Turbines. Copenhagen, Denmark, s.n.~~

~~BVG, 2025. Guide to a Floating Offshore Wind Farm, Swindon: BVG.~~

~~Campos, A., Molins, C., Trubat, P. & Alcaron, D., 2017. A 3D FEM model for floating wind turbines support structures. Trondheim, s.n.~~

~~Chatfield, C., 2020. Time-series forecasting. In: C. a. Hall/CRC., ed. s.l.:Taylor Francis.~~

~~Deb, K., 2000. An efficient constraint handling method for genetic algorithms. Computer methods in applied mechanics and engineering, 186(2-4), pp. 311-338.~~

Formatted: Heading 1

~~**Deb, K. & Agrawal, R., 1995. Simulated binary crossover for continuous search space. Complex systems, 9(2), pp. 115-148.**~~

~~**DNV, 2023. Energy Transition Outlook, Hovik: DNV.**~~

~~**Dou, S. et al., 2020. Optimization of floating wind turbine support structures using frequency-domain analysis and analytical gradients. s.l., Journal of Physics: Conference Series.**~~

~~**Driscoll, F. et al., 2016. Validation of a FAST Model of the Statoil-Hywind Demo Floating Wind Turbine. Trondheim, Norway, s.n.**~~

~~**Faraggiana, E. et al., 2022. An efficient optimisation tool for floating offshore wind support structures. Energy Reports, Volume 8, pp. 9104 - 9118.**~~

~~**Gaertner, E. et al., 2020. IEA Wind TCP Task 37: Definition of the IEA Wind 15-Megawatt Offshore Reference Wind Turbine (Technical Report), Golden, CO: National Renewable Energy Laboratory.**~~

~~**Hall, M., 2013. A cumulative Multi-Niching genetic algorithm for multimodal function optimization. arXiv preprint.**~~

~~**Hall, M., Buckham B & Crawford, C., 2013. Evolving Offshore Wind: A Genetic Algorithm-Based Support Structure Optimization Framework for Floating Wind Turbines. Bergen, Norway, s.n.**~~

~~**Hall, M. & Buckham, B., 2012. Genetic algorithm-based platform optimization for floating offshore wind turbines. Vancouver, Canada, Gene.**~~

~~**Hall, M., Housner, S., Zalkind, D. & Bortolotti, P., 2022. An Open-Source Frequency-Domain Model for Floating Wind Turbine Design Optimization. Delft, Netherlands, s.n.**~~

~~**Jacobsen, A. & Godvik, M., 2021. Influence of wakes and atmospheric stability on the floater responses of the Hywind Scotland wind turbines. Wind Energy, Volume 24, pp. 149-161.**~~

~~**Jacobsen, A. & Godvik, M., 2021. Influence of wakes and atmospheric stability on the floater responses of the Hywind Scotland wind turbines. Wind Energy, 24(2), pp. 149-161.**~~

~~**James, R. & Ros, M. C., 2015. Floating offshore wind: market and technology review, s.l.: The Carbon trust.**~~

~~Jin, B. & Xu, X., 2024. Predictions of steel price indices through machine learning for the regional northeast Chinese market. Neural computing and applications, 36(33), pp. 20863-20882.~~

~~Jonkman, J., Butterfield, S., Musial, W. & Scott, G., 2009. Definition of a 5-MW Reference Wind Turbine for Offshore System Development." (2009)., s.l.: National Renewable Energy Laboratory (NREL).~~

~~Katoch, S., Chauhan, S. & Kumar, V., 2021. A review on genetic algorithm: past, present, and future. Multimedia tools and applications, 80(5), pp. 8091-8126.~~

~~Liu, Y., Li, S., Yi, Q. & Chen, D., 2016. Developments in semi-submersible floating foundations supporting wind turbines: A comprehensive review. Renewable and Sustainable Energy Reviews, Volume 60, pp. 433-449.~~

~~Mareike, L. & Kolios, A., 2021. Reliability-based design optimization of a spar-type floating offshore wind turbine support structure. Reliability Engineering & System Safety, Volume 213.~~

~~Martini, M. et al., 2016. Met-ocean conditions influence on floating offshore wind farms power production. Wind Energy, 19(3), pp. 399-420.~~

~~Martins, J. R. R. A. & Ning, A., 2022. Engineering Design Optimization. Cambridge,: Cambridge University Press.~~

~~Messmer, T. et al., 2023. Overview of the potential of floating wind in Europe based on met-ocean data derived from the ERA5-dataset. s.l., Journal of Physics: Conference Series.~~

~~Musial, W., Butterfield, S. & Boone, A., 2004. Feasibility of Floating Platform Systems for Wind Turbines. Reno, Nevada, s.n.~~

~~Musial, W. et al., 2023. Offshore wind market report: 2023 edition, Golden, CO: National Renewable Energy Laboratory (NREL).~~

~~Myhr, A., Bjerkseter, C., Ågotnes, A. & Nygaard, T., 2014. Levelized cost of energy for offshore floating wind turbines in a life cycle perspective. Renewable Energy, Volume 66, pp. 714-728.~~

~~Otter, A., Murphy, J., Pakrashi, V. & Robertson, A., 2021. A review of modelling techniques for floating offshore wind turbines. Wind Energy, Volume 25, pp. 831-857.~~

~~Papi, F. & Bianchini, A., 2022. Technical challenges in floating offshore wind turbine upscaling: A critical analysis based on the NREL 5 MW and IEA 15 MW Reference Turbines. Renewable and Sustainable Energy Reviews, Volume 162.~~

~~Qiua, W. et al., 2008. Multi-objective optimization of semi-submersible platforms using particle swam optimization algorithm based on surrogate model. Ocean Engineering, Volume 178, pp. 388-409.~~

~~Risch, D. et al., 2023. Characterisation of underwater operational noise of two types of floating offshore wind turbines, s.l.: Scottish Association for Marine Science (SAMS).~~

~~Sergiienko, N. et al., 2022. Review of scaling laws applied to floating offshore wind turbines. Renewable and Sustainable Energy Reviews, Volume 162.~~

~~Skaare, B. et al., 2015. Analysis of measurements and simulations from the Hywind Demo floating wind turbine. Wind Energy, 18(6), pp. 1105-1122.~~

~~Tarsitano, A. & Amerise, I. L., 2017. Short-term load forecasting using a two-stage sarimax model. Energy, Volume 133, pp. 108-114.~~

~~Wang, T., Leung, H., Z. J. & Wang, W., 2020. Multiseries featural LSTM for partial periodic time-series prediction: A case study for steel industry. EEE Transactions on Instrumentation and Measurement, 69(9), pp. 5994-6003.~~

~~Wayman, E. et al., 2006. Coupled Dynamic Modeling of Floating Wind Turbine Systems. Houston, Texas, s.n.~~

~~Wu, j. & Kim, M.-H., 2021. Generic Upscaling Methodology of a Floating Offshore Wind Turbine. Energies, Volume 14.~~

~~Zalkind, D. & Bortolotti, P., 2024. Control Co-Design Studies for a 22 MW Semisubmersible Floating Wind Turbine Platform. Firenze, IOP Publishing Ltd.~~

~~Zhang, T. et al., 2023. Long-term energy and peak power demand forecasting based on sequential-XGBoost. IEEE Transactions on Power Systems, 39(2), pp. 3088-3104.~~

9 References

Formatted: Heading 1

Albulescu, C.T. (2021) ‘COVID-19 and the United States financial markets’ volatility’, Finance Research Letters, 38, 101699. https://doi.org/10.1016/j.frl.2020.101699.

Allen, C., Viselli, A., Dagher, H., Goupee, A., Gaertner, E., Abbas, N., Hall, M. and Barter, G. (2020) Definition of the UMaine VolturnUS-S Reference Platform Developed for the IEA Wind 15-Megawatt Offshore Reference Wind Turbine. Golden, CO: National Renewable Energy Laboratory. NREL/TP-5000-76773. https://doi.org/10.2172/1660012.

Bak, C., Zahle, F., Bitsche, R., Kim, T., Yde, A., Henriksen, L.C., Hansen, M.H., Blasques, J.P.A.A., Gaunaa, M. and Natarajan, A. (2013) The DTU 10-MW Reference Wind Turbine. Presented at Danish Wind Power Research 2013, Fredericia, Denmark, 27–28 May 2013.

Barter, G.E., Robertson, A. and Musial, W. (2020) ‘A systems engineering vision for floating offshore wind cost optimization’, Renewable Energy Focus, 34, pp. 1–16. https://doi.org/10.1016/j.ref.2020.03.002.

Beiter, P., Musial, W., Duffy, P., Cooperman, A., Shields, M., Heimiller, D. and Optis, M. (2020) The Cost of Floating Offshore Wind Energy in California Between 2019 and 2032. Golden, CO: National Renewable Energy Laboratory. NREL/TP-5000-77384; BOEM 2020-048.

Benifla, V. and Adam, F. (2023) ‘Design optimization of floating offshore wind turbine substructure using frequency-domain modelling and genetic algorithm’, Journal of Physics: Conference Series, 2626, 012047. https://doi.org/10.1088/1742-6596/2626/1/012047.

Beyer, F., Choisnet, T., Kretschmer, M. and Cheng, P.W. (2015) ‘Coupled MBS–CFD simulation of the IDEOL floating offshore wind turbine foundation compared to wave tank model test data’, in Proceedings of the 25th International Ocean and Polar Engineering Conference. Kona, Hawaii, 21–26 June 2015. International Society of Offshore and Polar Engineers.

Butterfield, S., Musial, W. and Jonkman, J. (2005) ‘Engineering challenges for floating offshore wind turbines’, in Proceedings of the Copenhagen Offshore Wind Conference. Copenhagen, Denmark.

BVG Associates (2025) Guide to a Floating Offshore Wind Farm. Swindon: BVG Associates.

Campos, A., Molins, C., Trubat, P. and Alarcón, D. (2017) ‘A 3D FEM model for floating wind turbine support structures’, presented at the EERA DeepWind Conference, Trondheim, Norway.

Chatfield, C. (2000) Time-Series Forecasting. Boca Raton, FL: Chapman & Hall/CRC. https://doi.org/10.1201/9781420036206.

Deb, K. (2000) ‘An efficient constraint handling method for genetic algorithms’, Computer Methods in Applied Mechanics and Engineering, 186(2–4), pp. 311–338. https://doi.org/10.1016/S0045-7825(99)00389-8.

Deb, K. and Agrawal, R.B. (1995) ‘Simulated binary crossover for continuous search space’, Complex Systems, 9(2), pp. 115–148.

DNV (2023) Energy Transition Outlook 2023. Høvik: DNV.

Dou, S., Pegalajar-Jurado, A., Wang, S., Bredmose, H. and Stolpe, M. (2020) ‘Optimization of floating wind turbine support structures using frequency-domain analysis and analytical gradients’, Journal of Physics: Conference Series, 1618(4), 042028. https://doi.org/10.1088/1742-6596/1618/4/042028.

Driscoll, F., Jonkman, J., Robertson, A., Sirnivas, S., Skaare, B. and Nielsen, F.G. (2016) ‘Validation of a FAST model of the Statoil-Hywind Demo floating wind turbine’, Energy Procedia, 94, pp. 3–19. https://doi.org/10.1016/j.egypro.2016.09.181.

Faraggiana, E., Sirigu, M., Ghigo, A., Bracco, G. and Mattiazzo, G. (2022) ‘An efficient optimisation tool for floating offshore wind support structures’, Energy Reports, 8, pp. 9104–9118. https://doi.org/10.1016/j.egyr.2022.07.036.

Gaertner, E., Rinker, J., Sethuraman, L., Zahle, F., Anderson, B., Barter, G., Abbas, N., Meng, F., Bortolotti, P., Skrzypinski, W., Scott, G., Feil, R., Bredmose, H., Dykes, K., Shields, M., Allen, C. and Viselli, A. (2020) IEA Wind TCP Task 37: Definition of the IEA 15-Megawatt Offshore Reference Wind Turbine. Golden, CO: National Renewable Energy Laboratory. NREL/TP-5000-75698. https://doi.org/10.2172/1603478.

Hall, M. (2013) ‘A cumulative multi-niching genetic algorithm for multimodal function optimization’, arXiv, arXiv:1304.0751. https://doi.org/10.48550/arXiv.1304.0751.

Hall, M., Buckham, B. and Crawford, C. (2013) ‘Evolving offshore wind: A genetic algorithm-based support structure optimization framework for floating wind turbines’, in OCEANS 2013 MTS/IEEE Bergen: The Challenges of the Northern Dimension. Bergen, Norway: IEEE, pp. 1–10. https://doi.org/10.1109/OCEANS-Bergen.2013.6608173.

Hall, M., Buckham, B. and Crawford, C. (2012) ‘A genetic algorithm-based platform optimization framework for floating offshore wind turbines’, presented at the 11th International Conference on Sustainable Energy Technologies, Vancouver, Canada.

Hall, M., Housner, S., Zalkind, D., Bortolotti, P., Ogden, D. and Barter, G. (2022) ‘An open-source frequency-domain model for floating wind turbine design optimization’, Journal of Physics: Conference Series, 2265(4), 042020. https://doi.org/10.1088/1742-6596/2265/4/042020.

Jacobsen, A. and Godvik, M. (2021) ‘Influence of wakes and atmospheric stability on the floater responses of the Hywind Scotland wind turbines’, Wind Energy, 24(2), pp. 149–161. https://doi.org/10.1002/we.2563.

James, R. and Costa Ros, M. (2015) Floating Offshore Wind: Market and Technology Review. London: The Carbon Trust.

Jin, B. and Xu, X. (2024) ‘Predictions of steel price indices through machine learning for the regional northeast Chinese market’, Neural Computing and Applications, 36(33), pp. 20863–20882. https://doi.org/10.1007/s00521-024-10270-7.

Jonkman, J., Butterfield, S., Musial, W. and Scott, G. (2009) Definition of a 5-MW Reference Wind Turbine for Offshore System Development. Golden, CO: National Renewable Energy Laboratory, NREL/TP-500-38060. https://doi.org/10.2172/947422.

Katoch, S., Chauhan, S.S. and Kumar, V. (2021) ‘A review on genetic algorithm: past, present, and future’, Multimedia Tools and Applications, 80(5), pp. 8091–8126. https://doi.org/10.1007/s11042-020-10139-6.

Liu, Y., Li, S., Yi, Q. and Chen, D. (2016) ‘Developments in semi-submersible floating foundations supporting wind turbines: A comprehensive review’, Renewable and Sustainable Energy Reviews, 60, pp. 433–449. https://doi.org/10.1016/j.rser.2016.01.109.

Leimeister, M. and Kolios, A. (2021) ‘Reliability-based design optimization of a spar-type floating offshore wind turbine support structure’, Reliability Engineering & System Safety, 213, 107666. https://doi.org/10.1016/j.ress.2021.107666.

Martini, M., Guanche, R., Armesto, J.A. and Losada, I.J. (2016) ‘Met-ocean conditions influence on floating offshore wind farms power production’, Wind Energy, 19(3), pp. 399–420.

Martins, J.R.R.A. and Ning, A. (2022) Engineering Design Optimization. Cambridge: Cambridge University Press. https://doi.org/10.1017/9781108980647.

Messmer, T., Hölling, M., Hegseth, J.M., Schlipf, D. and Peinke, J. (2023) ‘Overview of the potential of floating wind in Europe based on met-ocean data derived from the ERA5 dataset’, Journal of Physics: Conference Series.

Musial, W., Butterfield, S. and Boone, A. (2004) ‘Feasibility of Floating Platform Systems for Wind Turbines’, Proceedings of the 42nd AIAA Aerospace Sciences Meeting and Exhibit, Reno, NV, USA. https://doi.org/10.2514/6.2004-1007.

Musial, W., Spitsen, P., Beiter, P., Nunemaker, J. and Gevorgian, V. (2023) Offshore Wind Market Report: 2023 Edition. Golden, CO: National Renewable Energy Laboratory (NREL), NREL/TP-5000-89266.

Myhr, A., Bjerkseter, C., Ågotnes, A. and Nygaard, T.A. (2014) ‘Levelized cost of energy for offshore floating wind turbines in a life cycle perspective’, Renewable Energy, 66, pp. 714–728. https://doi.org/10.1016/j.renene.2014.01.017.

Otter, A., Murphy, J., Pakrashi, V. and Robertson, A. (2022) ‘A review of modelling techniques for floating offshore wind turbines’, Wind Energy, 25(5), pp. 831–857. https://doi.org/10.1002/we.2702.

Papi, F. and Bianchini, A. (2022) ‘Technical challenges in floating offshore wind turbine upscaling: A critical analysis based on the NREL 5 MW and IEA 15 MW reference turbines’, Renewable and Sustainable Energy Reviews, 162, 112489. https://doi.org/10.1016/j.rser.2022.112489.

Qiu, W., Wang, Y., Kim, C.W. and co-authors (2019) ‘Multi-objective optimization of semi-submersible platforms using particle swarm optimization algorithm based on surrogate model’, Ocean Engineering, 178, pp. 388–409. https://doi.org/10.1016/j.oceaneng.2019.03.007.

Risch, D., Sparling, C., McConnell, B., Wilson, B. and co-authors (2023) Characterisation of Underwater Operational Noise of Two Types of Floating Offshore Wind Turbines. Oban, UK: Scottish Association for Marine Science (SAMS).

Sergiienko, N., Cazzolato, B., Ding, B. and co-authors (2022) ‘Review of scaling laws applied to floating offshore wind turbines’, Renewable and Sustainable Energy Reviews, 162, 112490. https://doi.org/10.1016/j.rser.2022.112490.

Skaare, B., Nielsen, F.G., Hanson, T.D., Yttervik, R., Havmøller, O. and Rekdal, A. (2015) ‘Analysis of measurements and simulations from the Hywind Demo floating wind turbine’, Wind Energy, 18(6), pp. 1105–1122. https://doi.org/10.1002/we.1750.

Tarsitano, A. and Amerise, I.L. (2017) ‘Short-term load forecasting using a two-stage SARIMAX model’, Energy, 133, pp. 108–114. https://doi.org/10.1016/j.energy.2017.05.126.

Wang, T., Leung, H., Zhao, J. and Wang, W. (2020) 'Multiseries featural LSTM for partial periodic time-series prediction: A case study for the steel industry', IEEE Transactions on Instrumentation and Measurement, 69(9), pp. 5994–6003. https://doi.org/10.1109/TIM.2020.2967247.

Wayman, E.N., Sclavounos, P.D., Butterfield, S., Jonkman, J. and Musial, W. (2006) 'Coupled dynamic modelling of floating wind turbine systems', in Proceedings of the Offshore Technology Conference, Houston, Texas, 1–4 May 2006. https://doi.org/10.4043/18287-MS.

Wu, J. and Kim, M.-H. (2021) 'Generic upscaling methodology of a floating offshore wind turbine', Energies, 14(24), 8490. https://doi.org/10.3390/en14248490.

Zalkind, D. and Bortolotti, P. (2024) 'Control co-design studies for a 22-MW semisubmersible floating wind turbine platform', Journal of Physics: Conference Series, 2767(8), 082020. https://doi.org/10.1088/1742-6596/2767/8/082020.

Zhang, T., Zhang, X., Rubasinghe, O., Liu, Y., Chow, Y., Iu, H.H.-C. and Fernando, T. (2024) 'Long-term energy and peak power demand forecasting based on Sequential-XGBoost', IEEE Transactions on Power Systems, 39(2), pp. 3088–3104. https://doi.org/10.1109/TPWRS.2023.3289400

Formatted: Font: 8 pt